Chemistry Faculty Research and Publications　　　　　Chemistry, Department of

5-29-2020

Silver(I) and Copper(I) Complexes of Semi-Bulky Nitrogen-Confused C-Scorpionates

Denan Wang

Fathiya Jahan

Kristin J. Meise

Sergey Lindeman

James R. Gardinier

Silver(I) and Copper(I) Complexes of Semi-Bulky Nitrogen-Confused C-Scorpionates

Denan Wang
Department of Chemistry, Marquette University, Milwaukee, WI
Fathiya Jahan
Department of Chemistry, Marquette University, Milwaukee, WI
Kristen J. Meise
Department of Chemistry, Marquette University, Milwaukee, WI
Sergey V. Lindeman
Department of Chemistry, Marquette University, Milwaukee, WI
James R. Gardinier
Department of Chemistry, Marquette University, Milwaukee, WI

Abstract

Two new sterically demanding nitrogen-confused *C*-scorpionate ligands with a bis(3,5-diisopropylpyrazol-1-yl)methyl group bound to the 3- position of a normal pyrazole ($^HL^{iPr2}$) or an *N*-toluenesulfonyl pyrazole ($^{Ts}L^{iPr2}$) have been prepared. Reactions between the ligands ($^xL^{iPr2}$) and silver trifluoromethanesulfonate, AgOTf, gave four new compounds of the types [Ag($^xL^{iPr2}$)](OTf) (x = Ts, 1a; x

= H, 2a) or [Ag($^xL^{iPr2}$)$_2$](OTf) (x = Ts, 1b; x = H, 2b) depending on the initial metal:ligand ratio. Similarly, the reactions with [Cu(CH$_3$CN)$_4$](PF$_6$) produce four new compounds of the type [Cu($^xL^{iPr2}$)(CH$_3$CN)](PF$_6$) (x = Ts, 3a; x = H, 4a) or [Cu($^xL^{iPr2}$)$_2$](PF$_6$) (x = Ts, 3b; x = H, 4b). The solid-state structures of four derivatives (1a·acetone, 3a, 3b·CH$_2$Cl$_2$, and 4b·2THF) were determined by single-crystal X-ray diffraction while all complexes were characterized in CH$_3$CN solution by NMR spectroscopy and ESI(+) MS. The eight new complexes catalyze the aziridination of styrene. The copper complexes were generally (but not exclusively) more active catalysts than their silver counterparts.
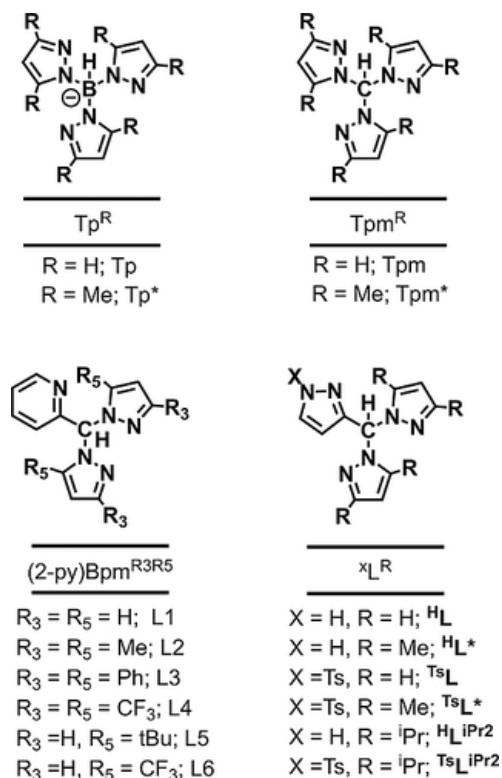
Abstract

The copper and silver complexes of bulky nitrogen-confused *C*-scorpionates were prepared to compare effects of ligand substitution, ligand number, and metal on their solid state and solution properties. The ability for the complexes to catalyze styrene aziridination with different nitrene sources was also evaluated.
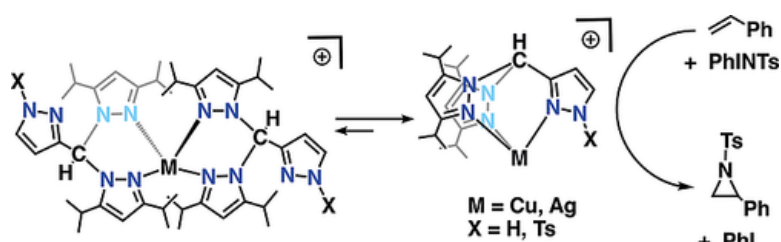
Introduction

Aziridines are important synthetic intermediates in organic synthesis, medicinal chemistry, and polymer chemistry[1, 2] Catalytic approaches to their syntheses have rapidly expanded in recent years.[1, 3-5] Transition metal-catalyzed reactions involving nitrene transfer to alkenes have gained prominence in this regard.[3, 5-9][10-19][20-27] Of these latter catalysts, copper(I) and silver(I) scorpionate complexes [tris(pyrazolyl)borates[14-17][28, 29] (normal scorpionates, or Tp^R, Scheme **1**, top left), tris(pyrazolyl)methanes (Tpm^R or *C*-scorpionates, Scheme **1**, top right),[30-32] certain C-heteroscorpionates (Scheme **1**, bottom left),[18] and certain nitrogen-confused C-scorpionates (Scheme **1**, bottom right)][27] have proven adept at catalytically affording aziridines from alkenes and various nitrene sources under mild conditions. Thus, Pérez and co-workers found that Tp*Cu(C$_2$H$_4$)[14, 17] or other CuTp^R complexes[15] (prepared in-situ) catalyze the aziridination of styrene, cyclooctene, or 1-hexene over the course of a few hours at room temperature in CH$_2$Cl$_2$ using PhI=NTs as a nitrene transfer agent. The CuTp^R could also catalyze aziridination using chloramine-T in CH$_3$CN to give more environmentally benign NaCl (vs. PhI) as a co-product.[15] Tp^{Br3}Cu(CH$_3$CN) was also found to catalyze nitrene transfer from PhI=NTs to furans in room temperature CH$_2$Cl$_2$ to give dihydropyridines.[33] AgTp* or Ag(Tp^{*,Br}) were found to be excellent catalysts for aziridination of styrenes, 2-alkenes, and even *E,E*-hexadien-1-ol in room temperature CH$_2$Cl$_2$ using PhI=NTs as a nitrene source.[16] For the latter substrate, the silver complexes offered higher regio- and stereoselectivity than their copper counterparts giving *trans*-aziridines vicinal to the alcohol group. Most recently, the Herres-Pawlis group[18] was able to trap and spectroscopically characterize the nitrene intermediates {[(2-py)Bpm^{R3R5}]Cu(NTs)}$^+$ in CH$_2$Cl$_2$ at −78 °C using (2-*t*BuSO$_2$)C$_6$H$_4$I=NTs[34] as a soluble nitrene source. The spectroscopic and magnetic data were consistent with diamagnetic, singlet species at −78 °C. Calculations showed ground state triplet but all spin states [$^{1/3}$Cu^I-nitrene or $^{1/3}$Cu^{II}-N·(iminyl)] and

nitrene binding modes ($\kappa^1 N$-, $\kappa^2 N,O$-) are thermally accessible. These intermediates were capable of stoichiometrically transferring a nitrene unit to a variety of substrates. Then, different {[(2-py)Bpm^{R3R5}]Cu(CH$_3$CN)}(PF$_6$) complexes were found to be capable catalysts for nitrene transfer to unsubstituted or p-substituted styrenes giving modest yields (> 65 %) of aziridine under mild ocnditions (PhI=NTs/CH$_2$Cl$_2$/295 K, 24 h).

Tp^R	Tpm^R
R = H; Tp	R = H; Tpm
R = Me; Tp*	R = Me; Tpm*

| (2-py)Bpm^{R3R5}	^{X}L^R
R$_3$ = R$_5$ = H; L1	X = H, R = H; ^{H}L
R$_3$ = R$_5$ = Me; L2	X = H, R = Me; ^{H}L*
R$_3$ = R$_5$ = Ph; L3	X =Ts, R = H; ^{Ts}L
R$_3$ = R$_5$ = CF$_3$; L4	X =Ts, R = Me; ^{Ts}L*
R$_3$ =H, R$_5$ = tBu; L5	X = H, R = ^{i}Pr; ^{H}L^{iPr2}
R$_3$ =H, R$_5$ = CF$_3$; L6	X =Ts, R = ^{i}Pr; ^{Ts}L^{iPr2}

Scheme 1 Structures and abbreviations of representative ligands referred to in this work. From left to right: scorpionate, C-scorpionate, C-heteroscorpionate, and nitrogen-confused C-scorpionate ligands. Ts = p-toluenesulfonyl.

In a previous study,[27] eight complexes of the type [Ag(^{X}L^R)$_n$](OTf) (n = 1, 2 and ^{X}L^R = ^{H}L, ^{Ts}L, ^{H}L*, and ^{Ts}L*) were characterized and evaluated for their ability to catalyze aziridination of styrene. Both ESI(+) MS and NMR spectroscopic studies indicated that the analytically pure [Ag(^{X}L^R)$_n$](OTf) compounds did not retain their structure in CH$_3$CN rather were involved in multiple dynamic equilibria in solution. These dynamic processes remained in the fast exchange regime on the NMR timescale down to the freezing point of the solvent, thereby obfuscating structural information. These silver complexes of nitrogen-confused C-scorpionates showed no or very little capacity to participate in styrene aziridination using PhI=NTs in room temperature CH$_2$Cl$_2$. However, [Ag(^{X}L^R)$_n$](OTf) showed modest catalytic activity at 80 °C in CH$_3$CN when employing a nitrene generated in-situ from H$_2$NTs and PhI(OAc). Interestingly, the bulkiest derivative [Ag(^{Ts}L*)$_2$](OTf) was reported to have the highest activity giving 34 % yield of the desired N-tosyl aziridine. This observation prompted the current study to determine if further increasing steric bulk of the ligands would lead to an increase in catalytic activity of silver complexes. Herein we report on the preparation of two new semi-bulky nitrogen confused scorpionates, ^{Ts}L^{iPr2} and ^{H}L^{iPr2} and their silver(I) and copper(I) complexes. The copper(I) complexes were prepared to compare catalytic activity with their silver congeners, and possibly to demonstrate the

generality of any trends in ligand sterics on catalytic activity. It was also hoped that the slower ligand exchange rates associated with the smaller copper(I) compared to silver(I) would give more informative NMR spectra to shed light on possible solution structures of the d^{10} metal complexes. During the course of study, we found the reported activity of [Ag(^{Ts}L*)$_2$](OTf) to be in error, and outline a more reliable protocol and data for this series of complexes.

Results and Discussion

The optimized synthetic route to the new bulky "confused" scorpionate ligands is outlined in Scheme **2**. The cobalt(II)-catalyzed Peterson rearrangement reaction[35-38] between *N*-tosylpyrazole-3-carboxaldehyde**39** and an excess of in-situ formed bis(3,5-diisopropylpyrazolyl)sulfinyl, O=S(pz^{iPr2})$_2$, gave very high yields (> 90 %) of the *N*-tosyl-protected ligand, ^{Ts}L^{iPr2}. The use of excess O=S(pz^{iPr2}) ensured reproducibly high yields. The ligand ^{Ts}L^{iPr2} could also be obtained in lower yields (ca. 65 %) in a multi-pot reaction using O=C(pz^{iPr2})$_2$ in toluene instead of the sulfinyl derivative in THF. As dipyrazolylcarbonyls are generally more reactive than their sulfinyl counterparts,[36] the lower yield by this latter route was initially surprising. It is noted, however, that the syntheses of O=C(pz^{iPr2})$_2$ from triphosgene and H(pz^{iPr2}) was invariable complicated by a small amount (ca. 5 %) of the starting heterocycle that is difficult to separate and likely interferes with the subsequent rearrangement reaction. The *N*-tosyl group of ^{Ts}L^{iPr2} was quickly and quantitatively hydrolyzed under basic conditions to give ^{H}L^{iPr2}.
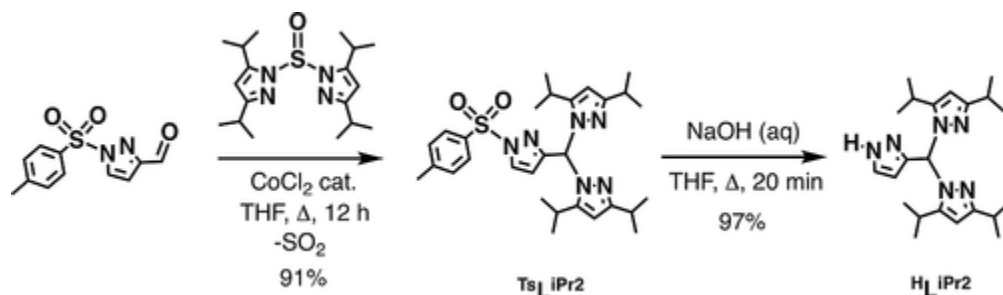
Scheme 2 Optimized route to the new C-scorpionate ligands.

The ^{1}H NMR spectrum of each ligand reveals a similar low symmetry. Specifically, there is only one resonance near δ_H = 6 ppm for the ring H$_4$-pz^{iPr2} hydrogen and two septet resonances near δ_H = 3.3 (J = 6.8 Hz) and 2.9 (J = 6.9 Hz) ppm for the CHMe$_2$ groups indicating equivalency of these two pyrazolyl rings, top right of Figure **1**. However, there are three doublet resonances near δ_H = 1.1, 1.0, 0.9 ppm that integrate to 12, 6, and 6 hydrogens for the isopropyl methyl groups. Moreover, the ^{13}C NMR shows 6 resonances for isopropyl group carbons. The observed number of resonances is unusual, since a C_s-symmetric ligand would be expected to give only two doublet *i*Pr-CH$_3$ ^{1}H resonances and four singlet ^{13}C isopropyl carbon resonances. Alternatively, as illustrated in Figure **1**, a C_1- symmetric species with free rotation of isopropyl groups and of pyrazolyl rings is expected to give four doublet *i*Pr-CH$_3$ ^{1}H resonances and eight singlet ^{13}C isopropyl carbon resonances (for groups a–d, left of Figure **1**). Thus, the unusual number of resonances may occur if the local magnetic environment becomes progressively equivalent (pseudo-C_2 symmetric) with increasing distance from the prochiral methine carbon, α, causing the resonances for isopropyl (and H$_4$/C$_4$ pyrazolyl) groups (a and b, Figure **1**) to have coincidental chemical shifts.
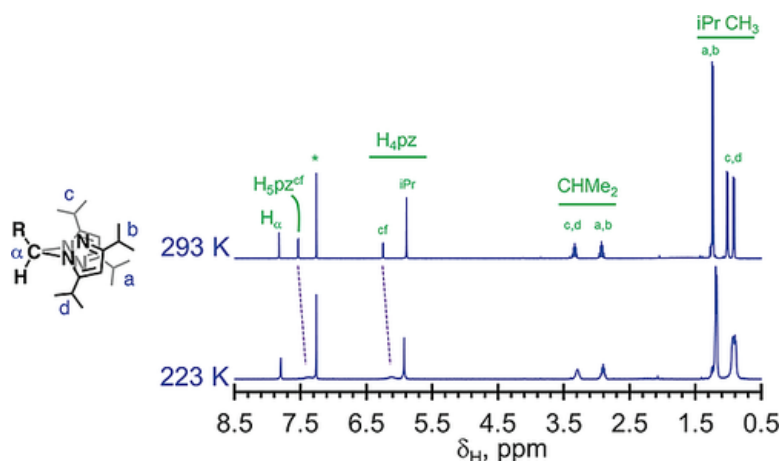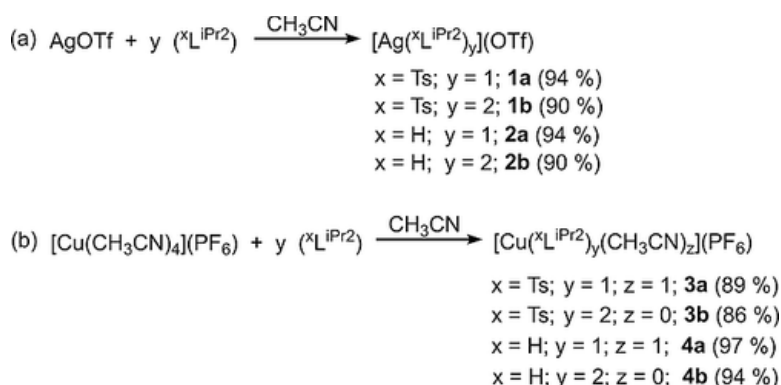
Figure 1 Left: Line drawing of a possible C_1-symmetric ligand geometry (R = ^{H}pz or ^{Ts}pz) with methine carbon and different isopropyl groups labeled. Right: ^{1}H NMR spectra of $^H L^{iPr2}$ in CDCl$_3$ at 293 K (top) and 223 K (bottom). The asterisk is for solvent resonance, the "cf" refers to the confused pyrazolyl ring hydrogens.

An alternate geometry with a C_s-symmetric ligand (with eclipsed diisopropyl pyrazolyl rings) and with 5- (but not the 3-) isopropyl groups locked into one position seems less likely since such an arrangement with overlapping nitrogen lone pairs on adjacent rings is energetically less favorable than a geometry like that in Figure **1**. Moreover, the unique proton of the proposed 5-*i*Pr CHMeMe' group is expected to appear as a quartet of quartets rather than the observed septet. The low temperature ^{1}H NMR spectrum of the ligands in CDCl$_3$ shows that the free rotation of the confused pyrazolyl slows into the intermediate exchange region near 223 K as the pyrazolyl doublet resonances broaden and shift upfield (bottom right Figure **1**). Concomitantly, the resonances for the 5-*i*Pr group hydrogens (the septet near 3.3 ppm and the two upfield doublets) broaden and shift upfield compared those in the high temperature spectrum. Unfortunately, the slow exchange limit is not reached before the solvent freezing point. The slow exchange limit was not even observed in the spectrum for CD$_2$Cl$_2$ solutions on cooling to 183 K.

Four silver(I) trifluoromethanesulfonate and four copper(I) hexafluorophosphate complexes were prepared in high yields (> 85 %) by direct addition of either one or two equivalents of ligands to the metal salts in CH$_3$CN according to Scheme **3**. After drying under vacuum, the mono- ligated silver complexes analyze as solvent-free [Ag($^x L^{iPr2}$)(OTf)] where x = *p*-toluenesulfonyl = Ts, 1a, or x = H, 2a, whereas the monoligated copper(I) complexes retain a molecule of acetonitrile to give [($^x L^{iPr2}$)Cu(CH$_3$CN)](PF$_6$) where x = *p*-toluenesulfonyl = Ts, 3a, or x = H, 4a. The difference in composition likely reflects the greater metal binding affinity of the triflate vs. hexafluorophosphate anion. Each of the diligated complexes [Ag($^x L^{iPr2}$)$_2$](OTf) (x = Ts, 1b, or x = H, 2b) or [Cu($^x L^{iPr2}$)$_2$](PF$_6$) (x = Ts, 3b, or x = H, 4b) is solvent free. The silver complexes were also prepared using THF as a solvent with generally good yields (> 80 %) but care was needed in workup to achieve these reasonably high yields reproducibly. Many silver complexes of tris(pyrazolyl)methanes are insoluble in THF so this solvent is generally used for their preparation. In this solvent, however, only 1b, gave a precipitate upon mixing reagents. The isopropyl groups confer considerable solubility to the silver complexes in THF, or even Et$_2$O (for 1a, 2a, 2b), so this method does not offer any advantage over preparations using CH$_3$CN.

(a) AgOTf + y (^{x}L^{iPr2}) $\xrightarrow{\text{CH}_3\text{CN}}$ [Ag(^{x}L^{iPr2})$_y$](OTf)

x = Ts; y = 1; **1a** (94 %)
x = Ts; y = 2; **1b** (90 %)
x = H; y = 1; **2a** (94 %)
x = H; y = 2; **2b** (90 %)

(b) [Cu(CH$_3$CN)$_4$](PF$_6$) + y (^{x}L^{iPr2}) $\xrightarrow{\text{CH}_3\text{CN}}$ [Cu(^{x}L^{iPr2})$_y$(CH$_3$CN)$_z$](PF$_6$)

x = Ts; y = 1; z = 1; **3a** (89 %)
x = Ts; y = 2; z = 0; **3b** (86 %)
x = H; y = 1; z = 1; **4a** (97 %)
x = H; y = 2; z = 0; **4b** (94 %)

Scheme 3 Bulk preparation of metal complexes of the new scorpionate ligands.

Solid State

Two of the mono-ligated complexes, namely Ag(^{Ts}L^{iPr2})(OTf)·acetone, 1a·acetone, and [(^{Ts}L^{iPr2})Cu(CH$_3$CN)](PF$_6$), 3a, gave crystals suitable for single-crystal X-ray diffraction. Views of the structures of these complexes are found in Figure **2**, while Table **1** collects selected bond lengths and angles. The structure of 1a·acetone is comparable to the related complex Ag(^{Ts}L*)(OTf) reported previously.[27] That is, silver center in 1a·acetone is tetracoordinate via bonding to a $\kappa^3 N$- ligand and an oxygen (O3) of the triflate ion. The acetone solvate molecule is not bound to silver; rather it occupies channels parallel with the *a*-axis of the crystal. The Ag1–O3 distance of 2.275(1) Å in 1a·acetone is longer than the comparable distance of 2.224(2) Å in Ag(^{Ts}L*)(OTf). In 1a·acetone, the two diisopropyl pyrazolyls Ag–N bonds [Ag1–N12 2.366(2), Ag1–N22 2.335(2) Å; average 2.35(2) Å] are shorter than that associated with the "confused" pyrazolyl [Ag1–N2 2.415(2) Å]. This asymmetric binding mode is similar to that in Ag(^{Ts}L*)(OTf) where Ag–N$_{pz*}$ averaged 2.34(1) Å and Ag–N2 was 2.427(2) Å. The bond angles about silver in the AgN$_3$O coordination environment give a τ_δ parameter[40, 41] of 0.63 which puts the coordination polyhedron at the borderline between distorted tetrahedral ($\tau_\delta \approx 0.63$–0.9) and distorted saw horse ($\tau_\delta \approx 0.45$–0.63) geometries, slightly more tetrahedral than found for Ag(^{Ts}L*)(OTf) ($\tau_\delta = 0.61$).

(a)

(b)

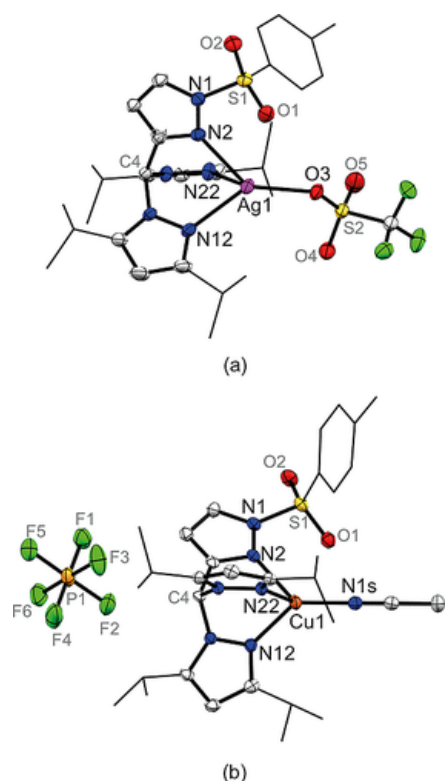**Figure 2** Structures of mono-ligated complexes (a) Ag($^{Ts}L^{iPr2}$)(OTf)·acetone, 1a·acetone and (b) [($^{Ts}L^{iPr2}$)Cu(CH$_3$CN)](PF$_6$), 3a, with atom labelling. Hydrogen atoms and minor disorder components of C14 and C16 in 1a·acetone are omitted for clarity.

Table 1. Bond lengths [Å] and angles [deg] for Ag($^{Ts}L^{iPr2}$)(OTf)·acetone, 1a·acetone and [($^{Ts}L^{iPr2}$)Cu(CH$_3$CN)](PF$_6$), 3a

1a·acetone		3a	
Bond lengths [Å]			
Ag1–N2	2.4150(15)	Cu1–N2	2.1800(13)
Ag1–N12	2.3664(18)	Cu1–N12	2.0447(13)
Ag1–N22	2.3345(15)	Cu1–N22	2.0920(13)
Ag1–O3	2.2745(13)	Cu1–N1s	1.8837(14)
Bond Angles [°]			
O3–Ag1–N2	128.20(5)	N1s–Cu1–N2	127.48(5)
O3–Ag1–N12	133.89(5)	N1s–Cu1–N12	132.61(5)
O3–Ag1–N22	135.92(5)	N1s–Cu1–N22	121.39(5)
N2–Ag1–N12	80.99(5)	N2–Cu1–N12	84.27(5)
N2–Ag1–N22	76.73(5)	N2–Cu1–N22	92.25(5)
N12–Ag1–N22	79.16(6)	N12–Cu1–N22	84.54(5)

The complex, [($^{Ts}L^{iPr2}$)Cu(CH$_3$CN)](PF$_6$), 3a, possesses a κ^3-ligand with a copper-bound acetonitrile molecule (Figure **2**b) to give a distorted tetrahedral CuN$_4$ kernel (τ_δ = 0.68). The average Cu–N(pyrazolyl), Cu–N$_{pz}$, distance of 2.11 Å is shorter than 2.12 Å found in the heteroscorpionate complex {[HC(3,5-(CF$_3$)$_2$pz)$_2$(Py)]Cu(CH$_3$CN)}(PF$_6$),**18** similar to 2.11 Å found in

{[HC(pz^{3tBu})$_3$]Cu(CH$_3$CN)}(PF$_6$),**42** but longer than 2.09 Å found in either {[HC(3,5-^{iPr2}pz)$_3$]Cu(CH$_3$CN)}(ClO$_4$)**43** or [(HC(pz$^{3-mesityl}$)$_3$)Cu(CH$_3$CN)]$_2$(Cu$_2$I$_4$).**44** The Cu–N(acetonitrile) distance of 1.884(1) Å in 3a is within the 1.86–1.89 Å range found in other complexes of the type {[tris(pyrazolyl)methane]Cu(CH$_3$CN)}$^+$.**42-44** Finally, it is noted that the PF$_6$ anion is docked close to the acidic methine and the confused pyrazolyl's H$_4$-ring hydrogen by two short CH···F weak hydrogen bonding**45-49** interactions (C2H2···F1 2.434 Å, 160.7° and C4H4···F3 2.480 Å, 151.9°, respectively).

The structures of two di-ligated complexes [Cu(^{Ts}L^{iP2r})$_2$](PF$_6$)·CH$_2$Cl$_2$, 3b·CH$_2$Cl$_2$, and [Cu(^{H}L^{iP2r})$_2$](PF$_6$)·2THF, 4b·2THF, are given in Figure **3**a and b, respectively. Selected interatomic distances and angles are collected in Table **2**. Despite the differences in substituents bound to the confused pyrazolyl N1 ring atom, the local structures of the cations in 3b·CH$_2$Cl$_2$, and 4b·2THF are quite similar. In each, the ligands are bound to copper(I) in a κ^2- fashion via the 3,5-diisopropylpyrazolyl donors; the "confused" pyrazolyl moieties are not bound to the metal. The CuN$_4$ kernel is best described as a distorted sawhorse by virtue of the combination of a borderline τ_δ value of 0.63 and C$_2$-symmetry (exact for 4b·2THF and approximate C$_2$ for 3b·CH$_2$Cl$_2$) that arises from two disparate sets of Cu–N$_{pz}$ distances. That is, in the distorted sawhorse approximation, the two pseudoequatorial Cu–N$_{pz}$ bonds are longer than 2.0 Å while the pseudoaxial bonds are shorter than 2.0 Å, where the average distance of the four Cu–N$_{pz}$ bonds is 2.045(2) Å for 3b·CH$_2$Cl$_2$ and 2.04(4) for 4b·2THF. The cation coordination geometry in each closely resembles those found in [Cu(H$_2$Cpz$_2$)$_2$](ClO$_4$) (avg. Cu–N$_{pz}$ 2.065 Å, τ_δ = 0.57),**50** or {Cu[H$_2$C(3,5-^{iPr2}pz)$_2$]$_2$}(X) (X = Cu^{I}Cl$_2$, avg. Cu–N$_{pz}$ 2.080 Å, τ_δ = 0.67; X = ClO$_4$, avg. Cu–N$_{pz}$ 2.068 Å, τ_δ = 0.64).**51** Finally, it is noted that in 3b·CH$_2$Cl$_2$ the PF$_6^-$ anion has CH···F weak hydrogen bonding interactions**45-49** with the acidic methine hydrogen (C44H44···F4 2.582 Å, 149.4°), the unique isopropyl hydrogen of groups attached to the 5-pyrazolyl positions adjacent to the methine (C50H50···F4 2.579 Å, 140.1°; C50H50···F6 2.565 Å, 120.0°; C10H10···F2 2.557 Å, 148.1° C20H20···F2 2.627 Å, 146.2°) and a 3-tolyl ring hydrogen (C35H35···F6 2.489 Å, 147.0°). In 4b·2THF, the PF$_6$ anion bridges neighboring cations via bifurcated C$_2$-symmetric N-H···F···H-N weak hydrogen bonding interactions (N1H1n···F2 2.343 Å, 138.0°) that gives chains of complexes parallel with the crystallographic *a*-axis (Figure S1).
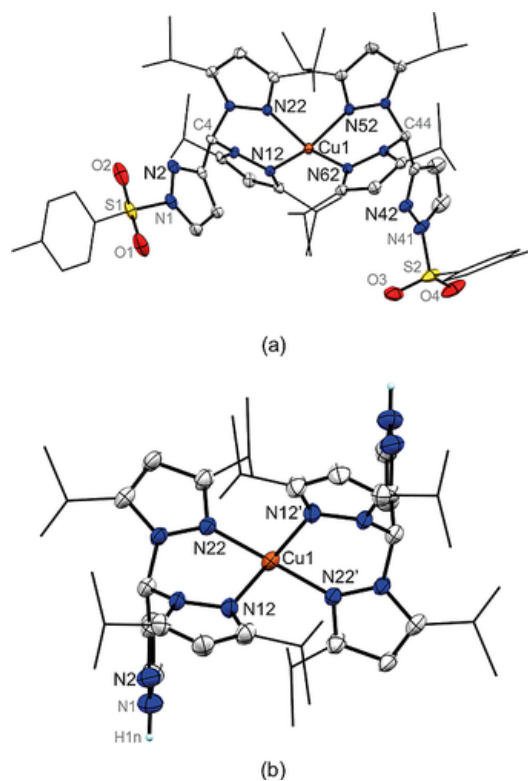
Figure 3 Views of the cation in (a) [Cu(^{Ts}L^{iPr2})$_2$](PF$_6$)·CH$_2$Cl$_2$, 3b·CH$_2$Cl$_2$, and (b) [Cu(^{H}L^{iPr2})$_2$](PF$_6$)·2THF, 4b·2THF, with partial atom labeling. Anions, solvate molecules and most hydrogens are omitted for clarity.

Table 2. Selected bond lengths [Å] and angles [deg] for [Cu(^{Ts}L^{iPr2})$_2$](PF$_6$)·CH$_2$Cl$_2$, 3b·CH$_2$Cl$_2$, and [Cu(^{H}L^{iPr2})$_2$](PF$_6$)·2THF, 4b·2THF

3b·CH$_2$Cl$_2$		4b·2THF	
Bond lengths [Å]			
Cu1–N12	1.9995(15)	Cu1–N12	2.088(3)
Cu1–N22	2.0760(15)	Cu1–N22	1.988(3)
Cu1–N52	2.1276(15)		
Cu1–N62	1.9763(15)		
Bond Angles [°]			
N62–Cu1–N12	137.88(6)	N12–Cu1–N22	94.07(12)
N62–Cu1–N22	113.69(6)	N12–Cu1–N12'	102.1(2)
N62–Cu1–N52	94.34(6)	N12–Cu1–N22'	111.88(12)
N12–Cu1–N22	93.23(6)	N22–Cu1–N22'	138.7(2)
N12–Cu1–N52	111.46(6)		
N22–Cu1–N52	102.46(6)		

Solution Behavior

When the analytically pure powders or crystals of the new compounds are dissolved in acetonitrile a mixture of species is formed due to multiple equilibria, a property that is evident from ESI(+) mass spectrometric and NMR spectroscopic data. First, electrospray mass spectrometry utilizes soft ionization such that this technique is not only useful for sampling the solution structure of inert

complexes,[52], [53] but can also be used to probe the solution behavior of labile metal complexes or even supramolecular species held together by non-covalent interactions.[54-57] When either analytically pure 1a or 1b are dissolved CH_3CN (with added formic acid), the mass spectrum consist of peaks for $[Ag(^{Ts}L^{iPr2})_2]^+$, $[Ag(^{Ts}L^{iPr2})]^+$, and $[H(^{Ts}L^{iPr2})]^+$ as well as a ligand fragmentation peak $[^{Ts}L^{iPr2} - pz^{iPr2}]^+$ where the relative abundance of each ion varied sample to sample. Similar data were found for the $^{H}LiPr$ derivatives, 2a or 2b. When CH_3CN/formic acid solutions of either 3a, 3b, 4a, or 4b were analyzed, the ESI(+) spectra showed peaks for $[Cu(^{x}L^{iPr2})_2]^+$, $[Cu(^{x}L^{iPr2})(CH_3CN)_n]^+$ (n = 0,1), $[H(^{x}L^{iPr2})]^+$, $[^{x}L^{iPr2} - pz^{iPr2}]^+$, and, in the cases of 3b or 4a, $[Cu(CH_3CN)_2]^+$. All of the above data, but especially the presence of $[M(^{x}L_2)]^+$ ions in solutions of analytically pure $[M(^{x}L^{iPr2})(CH_3CN)_n](OTf$ or $PF_6)$ (n = 0,1), indicate that the complexes do not remain intact in solution.

The ^1H and ^{13}C NMR spectroscopic data are also indicative of solution equilibria. The NMR spectra did not match expectations based on the respective solid-state structures (for 1a, 3a, 3b, and 4b) or molecular models (for 1b, 2a, 2b, or 4a); the spectra for the silver complexes were simpler while those for the copper derivatives were much more complex than expected. The major differences in the NMR spectra between analogous complexes of each metal is due, in part, to the greater exchange rate[58] of silver(I) (always in the fast exchange regime on the NMR time scale) vs. the copper(I) counterparts (which traverse the fast to slow exchange regime in the solvent's liquid range).

First, NMR titrations were performed by adding substoichiometric quantities of metal salt in CD_3CN to CD_3CN solutions of the various ligands at room temperature as well as by performing reverse titrations (adding substoichiometric quantities of ligand into an initial solution of ligand-free metal salt). The data for the latter are more or less identical to the former, so the former will be discussed. Overlays of the NMR spectra from titration experiments are given in Figures 4, 5, and S2 to S6. The number and chemical shifts of resonances indicate that complexes with 1:1 and 1:2 M/L stoichiometries are formed and that there is fast exchange between free ligands and complexes. As exemplified for the titration between $^{H}L^{iPr2}$ and AgOTf, in Figure 4, solutions with excess ligand (Figure 4b) or AgOTf (Figure 4f and g) with respect to complexes 2a/b gave only one set of resonances that show ligand exchange is fast on the NMR timescale. Moreover, a rapid equilibrium between silver containing species exists (vide infra) since the chemical shifts vary smoothly between limits found for 1:1 and 2:1 L/M stoichiometric ratios. The ^1H NMR spectrum of $[Ag(^{H}L^{iPr2})](OTf)$, 2a, (Figure 4e–g) shows that most resonances are shifted downfield from those in the free ligand (Figure 4a), as expected. Exceptions occur for the methine H_α resonance ($\delta_H \approx 7.5$ Figure 4a) and those resonances for one of the two sets of isopropyl groups near ($\delta_H \approx 3.0$ ppm Figure 4a and $\delta_H \approx 1.2$ ppm right of Figure 4). These exceptional resonances are shifted upfield from those in the free ligand by $|\Delta\delta|$ = 0.10 (H_α), 0.03 ($CHMe_2$), and 0.005 (iPr CH_3) ppm, respectively. The significant anomalous upfield shift of the former is thought to arise from close ion-pair contact with the triflate ion oxygen atoms, since similar behavior has been observed in solutions of other metal complexes[59-66] and because the triflate ion is often found to be in close contact with the methine hydrogen of the ligands in the solid state (including that of 1a·acetone).[67] It is noted that in solution the triflate ion in $[Ag(^{x}L^{iPr2})](OTf)$ is not bound to the metal, rather it is displaced by CD_3CN. The ^{19}F NMR spectrum of each of the four silver compounds is identical and shows only a single resonance at −79.3 ppm, a chemical shift that is identical to that in the spectrum of either NBu_4OTf, $[(\kappa^3N-^{x}L^*)Mn(CO)_3](OTf)$ (x = Ts, H),[27] or $[Fe(\kappa^3N-^{H}L)_2](OTf)_2$,[39, 68] species with "free" triflate ions. Ion-pairing of triflate with cations has minimal effect on the chemical shift of the ^{19}F resonance

because the ion pair contact occurs only with the oxygen atoms. The ^{1}H NMR spectrum of 1a is similar to that of 2a, but the resonance for H$_4$ of the confused ring (nearest to the methine H$_\alpha$) and the resonances for the tolyl ring hydrogens are also shifted upfield with respect to the free ligand; the tolyl CH$_3$ resonance is unchanged. Additionally, there is only one set of resonances for diisopropylpyrazolyl hydrogens indicating that the tosyl group must rapidly rotate to average the signals for the heterocycle hydrogens. If the solid-state structure was maintained with frozen C_1 point group symmetry, then two sets of resonances would be anticipated. The ^{1}H NMR spectra of the di-ligated complexes 1b and 2b are similar to the mono-ligated cases, but as shown for 2b in Figure 4c and the middle spectrum in the right of Figure 4, the H$_4$-pz^{cf} resonance ($|\Delta\delta|$ = 0.19 ppm) and one set of isopropyl resonances exhibit quite large upfield shifts with respect to the free ligand (CHMe$_2$ $|\Delta\delta|$ = 0.45 ppm; iPr-CH$_3$ $|\Delta\delta|$ = 0.19 ppm) while the upfield shift for the methine H$_\alpha$ resonance is modest ($|\Delta\delta|$ = 0.08 ppm). These features are qualitatively in agreement with those observed for previous [Ag(^{X}L*)$_2$](OTf) complexes,[27] which have κ^2N- ligands with non-bonded confused pyrazolyl rings in the solid state and possibly interconverting to κ^3N- ligands in solution due to low energy barriers for such conversions.[69, 70] Given the greater steric profile of diisopropyl pyrazolyls vs. dimethylpyrazolyls, it is likely that the current complexes 1b and 2b have κ^2N- rather than κ^3N- ligands in solution. Unfortunately, the exchange was still rapid even after lowering the temperature of the solution to 243 K, near the freezing point of the solvent. Thus, it was not possible to quantitatively evaluate the equilibrium constants or thermodynamic parameters for any of the dynamic equilibria, described by Equations 1–4. Qualitatively, the equilibrium constant for Equation 1 must be large (> 10^3) and that for Equation 3 must be small (< 10^{-3}) since the titration of ^{X}L with [Ag(CH$_3$CN)$_4$](OTf) (or the reverse titration) was complete at the stoichiometric limits.

$$[Ag(CH_3CN)_4)(OTf) + {}^XL \leftrightarrows [({}^XL)Ag(CH_3CN))(OTf) + 3\ CH_3CN$$
(1)

$$[({}^XL)Ag(CH_3CN)](OTf) + {}^XL \leftrightarrows [Ag({}^XL)_2)(OTf) + CH_3CN$$

(2)

$$2\ [({}^XL)Ag(CH_3CN)](OTf) + 2\ CH_3CN \leftrightarrows [Ag({}^XL)_2](OTf) + [Ag(CH_3CN)_4](OTf)$$

(3)

$$[({}^XL)\ Ag(CH_3CN))(OTf) \leftrightarrows ({}^XL)Ag(OTf)\ +\ CH_3CN$$

(4)
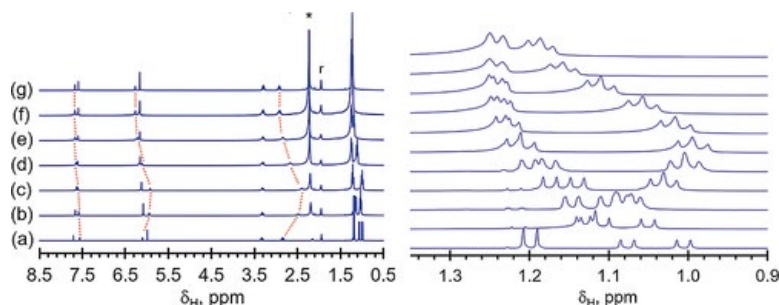
Figure 4 Left: Overlay of a portion of the ^1H NMR spectra obtained by titration of a concentrated CD_3CN solution of AgOTf into to a CD_3CN solution of $^HL^{iPr2}$. Molar equivalents of AgOTf added to $^HL^{iPr2}$: (a) zero; (b) 0.3; (c) 0.5; (d) 0.8; (e) 1.0; (f) 1.5; (g) 2.0. The doublet resonances for the confused pyrazolyl ring hydrogens and one multiplet resonance for a $CHMe_2$ group are tracked with orange dashed lines as a visual guide. The "r" represents residual CD_2HCN resonance while the asterisk "*" represents residual H_2O in CD_3CN. Right: Overlay of iPr-CH_3 region of the NMR spectrum of the free ligand (bottom) and after incremental additions of 0.1 equivalents of AgOTf until a 1:1 L/Ag ratio (top).
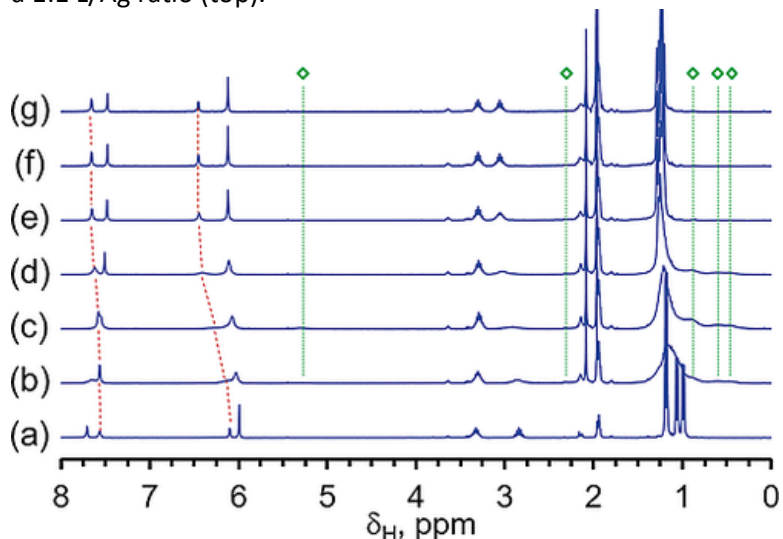
Figure 5 Portion of the 295 K ^1H NMR spectrum for a CD_3CN solution of $^HL^{iPr2}$ (a) before and after aliquots of $[Cu(CH_3CN)_4](PF_6)$ are added such as to give M/L ratios of: (b) 0.25, (c) 0.5, (d) 0.75, (e) 1.0, (f) 1.5, and (g) 2.0. The green diamonds and green dashed lines represent the unique resonances for $[Cu(^HL^{iPr2})_2]^+$ while the red dashed lines between 8 to 6 ppm follow resonances for confused pyrazolyl hydrogens assigned to $[(^HL^{iPr2})Cu(CH_3CN)]^+$. Resonances between 2.2 to 1.8 ppm are from solvent.
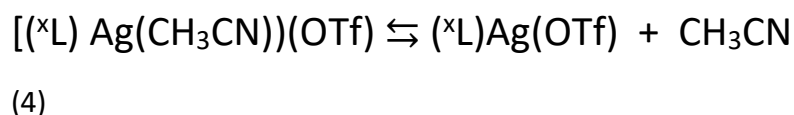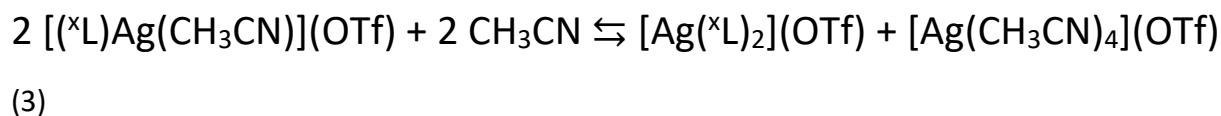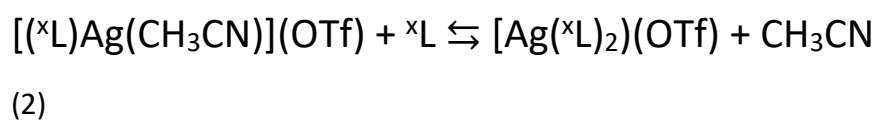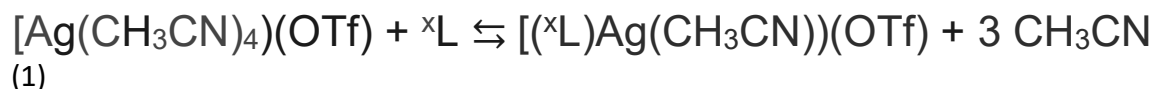
The NMR data for titration of $^xL^{iPr2}$ with $[Cu(CH_3CN)_4](PF_6)$ are more complicated than those of the silver analogues because the slower exchange rate associated with $Cu^{(I)}$ permits the observation of multiple species. An overlay of a portion of some of the spectra from titration experiments involving $^HL^{iPr2}$ is given in Figure **5** while full data are provided in Figure S5. Addition of substoichiometric portions of either $[Cu(CH_3CN)_4](PF_6)$ to a CD_3CN solution of $^HL^{iPr2}$ (Figure **5**) or of $^HL^{iPr2}$ to a CD_3CN solution of $[(^HL^{iPr2})Cu(CH_3CN)]^+$ (Figure S6) gives qualitatively similar spectra that consist of two sets of resonances of unequal intensity: the minor component corresponds to $[Cu(^HL^{iPr2})_2]^+$ while the major component of the spectra is due to $[(^HL^{iPr2})Cu(CH_3CN)]^+$ in fast exchange with free $^HL^{iPr2}$. It is noted that when analytically pure crystals of either 4a or 4b are dissolved in CD_3CN, the ^1H NMR spectra match those from titration experiments showing two unequal sets of resonances. In the former titration, both components are observed until an equimolar metal:ligand ratio is achieved. However, when the metal:ligand ratio is greater than one, then only resonances for $[(^HL^{iPr2})Cu(CH_3CN)]^+$ (in exchange with free $^HL^{iPr2}$) are clearly visible in the 295 K spectrum. As can be elucidated by comparing spectrum for the free ligand in Figure **5**a with those in Figure **4**e through 4g, most resonances for the ligand hydrogens in $[(^HL^{iPr2})Cu(CH_3CN)]^+$ are shifted downfield compared to those of the free ligand. Exceptions occur for the methine resonance at δ_H = 7.48 and the septet at δ_H = 3.30 ppm for one of the $CHMe_2$ hydrogens that are shifted upfield from those of the free ligand by $|\Delta\delta|$ = 0.23 and 0.03 ppm, respectively. Similar to the silver complexes described above, these upfield

shifts may be related to the proximity of the anion (hexafluorophosphate, in this case) to hydrogens on the cation. Fast exchange between the free and complexed ligand in [(^{H}L^{iPr2})Cu(CH$_3$CN)]$^+$ is indicated by two features of the NMR spectra. First, there is only one set of major resonances (i.e., momentarily disregarding those minor resonances for [Cu(^{H}L^{iPr2})$_2$]$^+$, vide infra) when either less than 0.5 equivalents [Cu(CH$_3$CN)$_4$](PF$_6$) are added to ^{H}L^{iPr2} (Figure **4**b–d) or when aliquots of free ligand are added to solutions of [(^{H}L^{iPr2})Cu(CH$_3$CN)]$^+$ (in the reverse titration, Figure S6). Second, the chemical shifts of these major resonances are weighted averages of those of [(^{H}L^{iPr2})Cu(CH$_3$CN)]$^+$ and the free ligand. At 295 K the resonances for [Cu(^{H}L^{iPr2})$_2$]$^+$ are broad and of weak intensity, with the characteristic ones demarcated by green diamonds and green dashed lines in Figure **5**. The broadness of the minor resonances arises because of dynamic molecular motion that falls in the slow to intermediate exchange rate regime at room temperature. Their weak intensity arises because of equilibria (vide infra) that favors [Cu(^{H}L^{iPr2})$_2$]$^+$ over [(^{H}L^{iPr2})Cu(CH$_3$CN)]$^+$ and ^{H}L^{iPr2} only at low temperature. The 243 K ^{1}H NMR spectrum of a 0.03 M solution of [Cu(^{H}L^{iPr2})$_2$](PF$_6$) in CD$_3$CN is shown in Figure **6**, while an overlay of ^{1}H NMR spectra acquired between 343 and 243 K are found in Figure S7. The major resonances for [Cu(^{H}L^{iPr2})$_2$]$^+$ are consistent with expectations based on the solid-state structure. That is, in the C$_2$-symmetric [Cu(^{H}L^{iPr2})$_2$]$^+$, there are two sets of diisopropylpyrazolyl rings; psuedoequatorial (top rings, colored green in Figure **6**) and pseudoaxial (bottom rings, colored blue in Figure **6**) and four sets of isopropyl groups (types A–D in Figure **6**). Inspection of the cation geometry in Figure **3**b and right of Figure **6** indicates that the 3-isopropyl groups nearest to the metal (types A and C) have close *intra*molecular contacts with pyrazolyl rings within the cation and are probably locked into position whereas the 5-isopropyl substituents only exhibit intermolecular contacts (see Table S3 for full details of noncovalent interactions). Moreover, the eight 3-isopropylpyrazolyl methyls are further subdivided into two sets, depending on whether the C-CH$_3$ bond is oriented either nearly parallel (A or C, Figure **6**, right) with or perpendicular (A' and C', Figure **6** right) to the C$_2$ rotation axis. The former reside above the pi clouds of the pyrazolyl rings whereas the latter do not. Thus, the ^{1}H NMR spectrum of [Cu(^{H}L^{iPr2})$_2$]$^+$, has three resonances for hydrogens of the confused pyrazolyl, one for the central methine hydrogen. The doublet for the H$_4$-ring hydrogen at δ_H = 5.42 ppm is significantly shifted upfield from that for the free ligand, presumably by contact with PF$_6^-$ ion. The two resonances near δ_H = 6 ppm are for the H$_4$-ring hydrogen of the pseudoequatorial and pseudoaxial diisopropylpyrazolyl rings. There are three resonances for the unique isopropylmethine hydrogens at δ_H = 3.3 (4 H, types B and D), 3.0 (2 H, type A) and 2.2 (2 H, type C) ppm. The tentative assignment of the most upfield resonance to the hydrogen of the C-type isopropyl group is based on the X-ray structure that shows that this hydrogen has a shorter C-H···π interaction[71-74] than the A-type hydrogen (C20H20···CtN1, 2.80 Å, 139° vs. C10H10···CtN22, 2.90 Å, 162°) while the other two hydrogens (types B and D) do not have intra or intermolecular short contacts. There are four resonances for isopropyl methyl hydrogens at δ_H = 1.2 (24 H), 0.9 (12 H), 0.6 (6 H), and 0.5 (6 H) ppm. The former resonance overlaps with the broad multiplet resonance(s) for [(^{H}L^{iPr2})Cu(CH$_3$CN)]$^+$ and the free ligand while the latter three are well resolved; the integration of the former (and percent composition of the mixture) is determined by the integration of these latter three resonances. Again the tentative assignment of the three upfield resonances is based on the metrics of intracationic C-H···π interactions (or long contacts at the van der Waals, vdW, limit), with the shortest (with type A shorter than type C, each with C-CH$_3$ bonds parallel with the two-fold rotation axis) having the greatest upfield shift. Given the relatively long distances of intracationic vdW contacts for methyls of types C, A',

and C', respectively, an alternate assignment where A' and C are switched in the spectrum shown in the left Figure **6** is possible. Regardless, the low temperature ^{1}H NMR spectrum is consistent with the solid-state structure of [Cu(^{H}L^{iPr2})$_2$]$^+$. Upon warming from 243 to 343 K, the resonances for [Cu(^{H}L^{iPr2})$_2$]$^+$, broaden, decrease in intensity and are no longer observed at about 323 K. At temperatures of 323 K or greater the ^{1}H NMR spectrum consists of one set of resonances for [(^{H}L^{iPr2})Cu(CH$_3$CN)]$^+$ in exchange with free ^{H}L^{iPr2}. Finally, as depicted in Figure S8 the relative amount of [Cu(^{H}L^{iPr2})$_2$]$^+$ vs. [(^{H}L^{iPr2})Cu(CH$_3$CN)]$^+$ and free ^{H}LiPr increases with initial concentration of [Cu(^{H}L^{iPr2})$_2$](PF$_6$) in CD$_3$CN, which is a consequence of the equilibria described below. In most respects, the ^{1}H NMR spectra for the ^{Ts}LiPr derivatives, 3a and 3b, are similar to those of 4a and 4b. However, the *N*-tosyl group not only gives more resonances but also slows the rate of dynamic motion such that the resonances for [Cu(^{Ts}L^{iPr2})$_2$]$^+$ are well-resolved at room temperature.
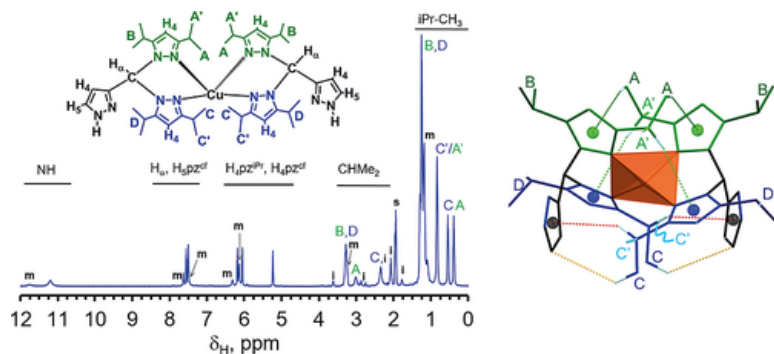
Figure 6 Left: The 243 K ^{1}H NMR spectrum of a 0.03 M solution of [Cu(^{H}L^{iPr2})$_2$](PF$_6$) in CD$_3$CN along with labeling diagram. The resonances marked with an "m" are for [(^{H}L^{iPr2})Cu(CH$_3$CN)]$^+$, that with an "s" is for residual solvent, and those with an "i" are from impurities in the deuterated solvent. Right: Partly labeled capped stick diagram of cation from X-ray structure with closest intracationic C-H···π interactions shown as dashed green, red, and orange lines and pyrazolyl ring centroids shown as spheres. Most of the hydrogens are removed except those involved in the noncovalent interactions. The atom coloring emphasizes spatial relationships of species in the line drawing to the left.

The NMR experiments indicate at least three equilibria determine the speciation of the copper(I) complexes in acetonitrile (Eq's 5–7). The first of the stepwise formation expressions (Equation 5) is thought to have a very large equilibrium constant ($K_5 > 10^5$) while that for the ligand redistribution reaction (Equation 7) is miniscule ($K \le 10^{-2}$) since the appropriate titrations (i.e., forward reaction of Equation 5 and reverse reaction of Equation 7) are complete at stoichiometric limits. The latter is corroborated by variable temperature NMR studies of [(^{x}L^{iPr2})Cu(CH$_3$CN)](PF$_6$) dissolved in CD$_3$CN for which the equilibrium constant associated with Equation 7, K_7, at 293 K for the tosyl derivative (x = Ts) was 1.2×10^{-4} with $\Delta H = -21$ kJ/mol and $\Delta S = -146$ J/K mol. The corresponding values for the ^{H}L^{iPr2} derivative were K_3 (293) = 3.2×10^{-3} with $\Delta H = -30$ kJ/mol and $\Delta S = -149$ J/K mol. As expected for Equation 7, the mono-ligated species is strongly entropically favored over the di-ligated species. The enthalpy change difference between the two ligand systems indicates stronger Cu–N$_{pz}$ bonding for [Cu(^{H}L^{iPr2})$_2$]$^+$ vs. [Cu(^{Ts}L^{iPr2})$_2$]$^+$ which might be expected on the basis of steric demands of the confused pyrazolyl N-substituent. The greater capacity for ^{H}LiPr to participate in weak N-H···F hydrogen bonding interactions with PF$_6$ anions may also contribute to the differences in enthalpy change. Finally, the titrations, variable temperature, and variable concentration NMR studies of pure [Cu(^{x}L^{iPr2})$_2$](PF$_6$)

dissolved in CD$_3$CN suggest that second stepwise formation expression (Equation 6) has a modest equilibrium constant, K_6, in the range of 10^2 to 10^3.

$$[Cu(CH_3CN)_4](PF_6) + {^x}L^{iPr} \leftrightarrows [(^xL^{iPr2})Cu(CH_3CN)](PF_6) + 3\ CH_3CN$$

(5)

$$[(^xL^{iPr2})Cu(CH_3CN)](PF_6) + {^x}L^{iPr2} \leftrightarrows [Cu(^xL^{iPr2})_2](PF_6) + CH_3CN$$

(6)

$$2\ [(^xL^{iPr2})Cu(CH_3CN)](PF_6) + 2\ CH_3CN \leftrightarrows [Cu(^xL^{iPr2})_2](PF_6) + [Cu(CH_3CN)_4](PF_6)$$
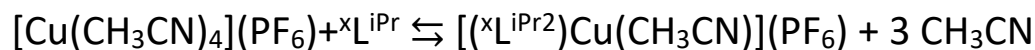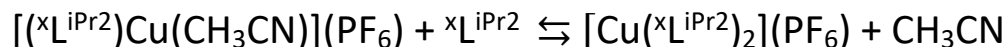
(7)

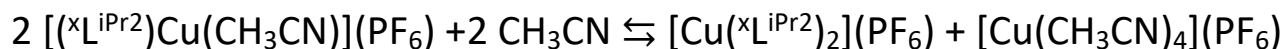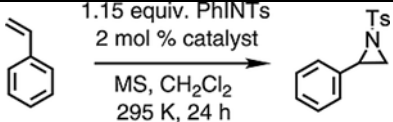That is, K_6 (293 K) for the $^{Ts}L^{iPr2}$ derivative was found to be 3.7×10^2 with $\Delta H = -19$ kJ/mol and $\Delta S = -16.0$ J/K mol while that for the $^HL^{iPr2}$ analogue is $2.5(2) \times 10^3$ at 293 K with $\Delta H = -21$ kJ/mol and $\Delta S = -5.5$ J/K mol. The enthalpic differences between complexes of the two different ligands likely arises because the larger steric demand of the former ligand destabilizes $[Cu(^{Ts}L^{iPr2})_2]^+$ over $[(^{Ts}L^{iPr2})Cu(CH_3CN)]^+$ by weakening the Cu–N$_{pz}$ bond to a greater extent than the $^HL^{iPr2}$ counterpart. The difference in steric demands of the ligands is likely the origin of the entropic difference where the loss of rotational/vibrational degrees of freedom of confused and/or isopropyl pyrazolyl groups upon on complexation to copper (compared to the free ligand) is greater for $^{Ts}L^{iPr2}$ than $^HL^{iPr2}$.

Catalysis

The ability of 1a, 1b, 2a, 2b, and related complexes to catalyze the aziridination of styrene was explored by using two methods, as summarized in Table **3** and Table **4**. Each entry of the tables is an average of at least two independent runs where the uncertainty is given in parentheses. First, in Method A, [(p-tolylsulfonyl)imino]phenyliodinane, PhI=NTs, was used as a nitrene source in CH$_2$Cl$_2$ at room temperature under heterogeneous conditions similar to that reported[18] for [Cu(2-py)Bpm^{R3R5}]-catalyzed reactions (direct comparisons of 6 mol-% catalyst loadings are found in Table **3**, entries 2, 8, 12, 16; otherwise 2 mol-% loadings were used). The second method (Method B) employed the nitrene formed in-situ from H$_2$NTs and PhI(OAc)$_2$ in CH$_3$CN at 80 °C, under conditions outlined by our previous study.[27] All of the complexes are capable of catalyzing the aziridination of styrene. The aziridination reactions do not occur to any significant extent in the absence of metal ion or complex. For Method A using PhI=NTs, the ligand free salts AgOTf or AgBF$_4$ were ineffective catalysts only giving a TON of 1 (entries 2 and 3, Table **3**) at 2 % loading and AgOTf had TON = 2 at 6 % loading. The silver C-scorpionate complexes outperformed the corresponding ligand-free silver salts with consistent but rather modest turnover numbers (TON) near 5 (entries 4–11, Table **3**) regardless of the number of ligands or type of pyrazolyl substituents. With a couple of exceptions described later, the copper complexes generally outperformed their silver counterparts. As found in entry 12 of Table **3**, the cuprous starting material [Cu(CH$_3$CN)$_4$]PF$_6$ outperformed all of the silver complexes with a TON of 11 at 2 mol-% loading. It is noted that when the loading was 6 mol-%, the TON only increased to 16; we were unable to achieve the reported TON of 26 despite numerous attempts. Also, given the substantial oxidizing power of PhI=NTs, the cupric salt Cu(OTf)$_2$ was investigated as a potential catalyst, but this species was less effective (TON = 3) than the cuprous starting material. In contrast to the silver complexes above, the

catalytic performance of the copper *C*-scorpionate complexes were dependent on ligand substitution patterns. Copper(I) complexes of the *N*-tosyl ligands ($^{Ts}L^*$, $^{Ts}L^{iPr2}$, Table **3**, entries 14–17) were the best catalysts of those tested with TONs between 25–29 for 2 % loading. When the catalyst loading was 6 mol-% for 3a (entry 17) the TON increased to 35 which is comparable to those reported[18] for the copper heteroscorpionates [Cu(L3 or L4)(CH$_3$CN)]PF$_6$ (see Scheme **1**) with TONs 31–32 under similar conditions. It is noted that, for $^{Ts}L^R$ complexes the nominally diligated species had the same (Table **3** entries 14 vs. 15) or only slightly better (entries 16 vs. 17) activities than the monoligated counterparts, which is reflective of ligand dissociation equilibria. On the other hand, the copper(I) complexes 4a and 4b with an N-H substituted ligand were equally ineffective with TON of 4 (entries 19 and 20). Finallly, it was found that the combination of Cu(OTf)$_2$ with two equivalents of $^{Ts}L^{iPr2}$ more than tripled the aziridination activity (giving a TON of 11) compared to the ligand-free cupric salt but was much less active than that involving its copper(I) counterpart 3b.

Table 3. Results of styrene aziridination reactions using PhI=NTs[a]

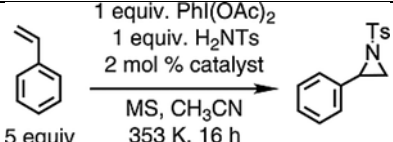| Entry	Catalyst	NMR % yield (±%)	TON[b]
1	None	< 1	–
2	Ag(OTf)	2(1), 5(1)d	1(1)
3	AgBF$_4$	2(1)	1(1)
4	[Ag($^{Ts}L^*$)](OTf)	10(1)c	5(1)
5	[Ag($^{Ts}L^*$)$_2$](OTf)	9(1), 9(1)c	5(1)
6	[Ag($^{H}L^*$)](OTf)	7(1)c	4(1)
7	[Ag($^{H}L^*$)$_2$](OTf)	8(1)c	4(1)
8	[Ag($^{Ts}L^{iPr2}$)](OTf), 1a	9(1),c 12(1)d	5(1)
9	[Ag($^{Ts}L^{iPr2}$)$_2$](OTf), 1b	8(1), 9(1)c	4(1)
10	[Ag($^{H}L^{iPr2}$)](OTf), 2a	8(1)c	4(1)
11	[Ag($^{H}L^{iPr2}$)$_2$](OTf), 2b	9(2)c	5(1)
12	[Cu(CH$_3$CN)$_4$](PF$_6$)	21(2), 31(2)d	11(1)
13	Cu(OTf)$_2$	5(1)	3(1)
14	[Cu($^{Ts}L^*$)(CH$_3$CN)](PF$_6$)	49(2)c	25(2)
15	[Cu($^{Ts}L^*$)$_2$](PF$_6$)	53(2)c	27(2)
16	[Cu($^{Ts}L^{iPr2}$)(CH$_3$CN)](PF$_6$), 3a	52(1), 53(1),c 69(1)d	26(1)
17	[Cu($^{Ts}L^{iPr2}$)$_2$](PF$_6$), 3b	58(2)c	29(2)
18	[Cu($^{Ts}L^{iPr2}$)$_2$](OTf)$_2$	22(1)c	11(1)
19	[Cu($^{H}L^{iPr2}$)(CH$_3$CN)](PF$_6$), 4a	8(2)c	4(2)
20	[Cu($^{H}L^{iPr2}$)$_2$](PF$_6$), 4b	7(2)c	4(1)

[a] Conditions: 0.5 mmol of styrene, 0.575 mmol of PhI=NTs, 0.01 mmol of catalyst, 0.5 g of 4 Å molecular sieves, 5 mL of CH$_2$Cl$_2$, 24 h, 23 °C.
[b] mmol aziridine/mmol catalyst reported for pre-formed catalysts (rather than in-situ formed catalysts unless data for the former not available).
[c] Catalyst formed in-situ.
[d] 6 mol-% catalyst.

Table 4. Results of styrene aziridination using PhI(OAc)$_2$/H$_2$NTs in CH$_3$CN[a]

Entry	Catalyst	NMR % yield (±%)	TON[b]
	1 equiv. PhI(OAc)$_2$; 1 equiv. H$_2$NTs; 2 mol % catalyst; MS, CH$_3$CN, 353 K, 16 h; 5 equiv styrene → Ts-aziridine		
1	None	3(2)	2(1)
2	Ag(OTf)	3(2)	2(1)
3	[Ag(^{Ts}L*)](OTf)	16(2), 15(2)c	8(3)
4	[Ag(^{Ts}L*)$_2$](OTf)	18(2), 16(2)c	9(2)
5	[Ag(^{Ts}L^{iPr2})](OTf), 1a	12(3), 15(2)c	6(2)
6	[Ag(^{Ts}L^{iPr2})$_2$](OTf), 1b	13(2), 9(2)c	7(1)
7	[Ag(^{H}L^{iPr2})](OTf), 2a	15(2), 16(1)c	8(1)
8	[Ag(^{H}L^{iPr2})$_2$](OTf), 2b	8(2), 10(2)c	4(1)
9	[Cu(CH$_3$CN)$_4$](PF$_6$)	61(2), 59(2)d	31(1)
10	Cu(OTf)$_2$	50(5)	25(3)
11	[Cu(^{Ts}L*)](PF$_6$)	65(4)c	33(2)
12	[Cu(^{Ts}L*)$_2$](PF$_6$)	59(3)c	30(2)
13	[Cu(^{Ts}L^{iPr2})(CH$_3$CN)](PF$_6$), 3a	67(2), 50(3)c	34(1)
14	[Cu(^{Ts}L^{iPr2})](OTf)$_2$	49(3)c	25(2)
15	[Cu(^{Ts}L^{iPr2})$_2$](PF$_6$), 3b	71(3), 50(2)c	36(2)
16	[Cu(^{Ts}L^{iPr2})$_2$](OTf)$_2$	40(2)c	20(1)
17	[Cu(^{H}L^{iPr2})(CH$_3$CN)](PF$_6$), 4a	61(3), 57(3)c	38(2)
18	[Cu(^{H}L^{iPr2})$_2$](PF$_6$), 4b	64(2), 59(2)c	30(1)

[a] Conditions: 5 mmol of styrene, 1 mmol of PhI(OAc)$_2$, 1 mmol of H$_2$NTs, 0.02 mmol of [Ag], 1 g of 4 Å molecular sieves, 4 mL of CH$_3$CN, 16 h, 80 °C.
[b] mmol aziridine/mmol catalyst, reported for pre-formed (rather than in-situ formed) catalysts unless data for the former not available.
[c] Catalyst formed in-situ.
[d] 1 mmol HOAc added.

In an effort to enhance product yield and to provide a comparison to an earlier study, the aziridination of styrene using method B (in-situ formed nitrene, 80 °C in CH$_3$CN) was pursued. The copper(I) complexes outperformed the corresponding silver(I) complexes. As might be expected from the difference in reaction temperatures, the yield of aziridine obtained from Method B was greater than Method A, but the improvement was modest being most significant for [Cu(CH$_3$CN)$_4$]PF$_6$, the cupric catalysts, or 4a or 4b, (compare Table **3** entires 12, 13, 18–20 with Table **4** entries 9. 10, 16–18). The reaction catalyzed by [Cu(CH$_3$CN)$_4$]PF$_6$ was found to be insensitive to either added acetic acid or a second equivalent of tosylamine. The drop-off in performance between cuprous and cupric salts (ca. TON 30 to 25, Table **3**, entrees 9 and 10) was not as substantial as in Method A which might be related to the ability of CH$_3$CN (vs. CH$_2$Cl$_2$) to potentially induce disproportionation and stabilize copper(I) over copper(II). Interestingly, the copper complexes only showed a marginal increase in catalytic activity vs. ligand-free copper salts. Moreover, there was little or no differentiation in the catalytic performance of the monoligated vs. diligated copper(I) complexes. So, ligand dissociation equilibria is likely responsible

for the catalytic activity of $[Cu(^XL^R)_2]^+$ and the rather modest performance increase of $[Cu(^XL^R)(CH_3CN)]^+$ vs. ligand-free salt. It is also noted that for the copper catalyzed reactions performed using Method B but in the absence of molecular sieves, the yields of aziridine product decrease because a sacrificial [3+2] cycloaddition reaction occurs between styrene and 2-phenyl-N-tosylaziridine to produce variable amounts of 2,4- diphenyl-N-tosylpyrrolidine (as a diastereomeric mixture)[75] where the yields of aziridine and pyrrolidine are generally 40 ± 7 % and 30 ± 4 %, respectively. This pyrrolidine by-product was previously observed, albeit in very minor amounts (1–2 %), in $[Ag(^XL^R)_n]^+$ catalyzed reactions.[27] It is unclear how molecular sieves suppress the cycloaddition reaction. Moreover, this side reaction is not found using Method A (with or without molecular sieves). Finally, although relatively modest, the catalytic activity of the silver complexes increases between two- to ten-fold over the ligand-free silver salt, AgOTf. Within experimental error, all of the silver catalysis performed equally regardless of number of C-scorpionate ligands or their substituents. It is noteworthy that the newly acquired results for $[Ag(^{Ts}L*)_2](OTf)$ (Table **4**, entry 4), differ from the erroneous results reported previously by our group [NMR yield 34(4), 27(3) (in-situ formed), TON 15]. By using several NMR standards [1,3,5-$(MeO)_3C_6H_3$, CH_3NO_2 and $SiMe_4$ spiked $CDCl_3$ solutions] and careful observation, it was found that the original standard p-$(Me_3Si)_2C_6H_4$ will partially sublime (artificially raising yields) from the crude mixture if a sample is subjected to an oil pump vacuum (10^{-4} Torr) while being heated by an external (70 °C) oil bath over the course of an hour (or more), in an effort to assist in solvent removal. Sublimation does not occur when solvent is simply removed at room temperature. Fortunately, the error only affected the anomalous result for $[Ag(^{Ts}L*)_2](OTf)$; the results of other complexes were reproducible (and low). Moreover, the new procedure described in the current experimental of using aliquots from stock solutions, minimizes errors in weighing small masses of catalysts. Finally it is noted that the Method B aziridination reactions were quite temperature sensitive. When reactions were performed at room temperature, instead of 80 °C, the yields of N-tosylaziridine obtained using copper catalysts dropped to approximately 25 % of the values reported in Table **3** while those using the silver complexes as potential catalysts failed provide any product.

The reactivity screening of the current complexes suggests that in addition to ligand dissociation, electronic factors are important in determining the efficacy of nitrene transfer reactions mediated by group 11 C-scorpionate complexes. For instance, the catalytic activity trends with the electron richness of the copper complexes supported by normal vs. C-scorpionates[43] {e.g., $E_{1/2}$ (Cu^{2+}/Cu^+) = 0.07 V, 0.43 V, 0.63 and 1.0 V vs. Ag/AgCl in CH_3CN for $CuTp^{iPr2}(CH_3CN)$, $[Cu(Tpm^{iPr2})(CH_3CN)]^+$, $[Cu(^{Ts}L^{iPr2})(CH_3CN)]^+$, and $[Cu(CH_3CN)_4]^+$,[76] respectively}. This trend appears to be further extended if one were to include the silver complexes, whose oxidation potentials are expected to be much higher [$E_{1/2}$ (Ag^{2+}/Ag^+) ≥ 1.6 V vs. Ag/AgCl[77-79]] than the copper derivatives. In the silver cases, the highly oxidative nature of any hypervalent iodine reagent {$E_{1/2}$ [$PhI(OAc)_2$/PhI] 2.2 V vs. Ag/AgCl[79]}, putative silver nitrene, or other unidentified $Ag^{(II)}$ intermediate may lead to oxidative decomposition of styrene [$E_{1/2}$ (styrene$^+$/styrene) 2.0 V vs. Ag/AgCl,[80]], or possibly of ligand, at a rate that becomes competitive with nitrene transfer, thereby reducing yields. Thus, as evident from relative $M(^XL^R)^{2+}/M(^XL^R)^+$ redox potentials (Table S4), the superiority of the copper(I) complexes over the silver relatives to effect aziridination of styrene might be traced to the enhanced stability of the metal nitrene intermediate brought about by copper's superior ability to back donate electrons into the un- or partly-filled orbitals on the unsaturated nitrogenous fragment (giving a bond with some metal-iminyl character). Unfortunately, it has not yet

proven possible to identify any group 11 nitrene intermediates supported by these $^xL^R$ ligands using PhI=NTs. However, it can speculated on the basis of VT NMR data of the starting metal complexes, the elevated temperatures required for aziridination in CH_3CN, and the structural similarity with {[(2-py)Bpm^{R3R5}]Cu}$^+$, that [($\kappa^{(3-n)}N$-$^xL^R$)(CH_3CN)$_n$M(NTs)]$^+$ (n = 0–2), are candidates for the catalytically active species. For the diligated complexes, it is not yet possible to exclude either [(κ^2-$^xL^R$)(κ^1-$^xL^R$)M(NTs)]$^+$ or [(κ^1-$^xL^R$)$_2$M(NTs)]$^+$, as the catalytically active species, although this seems less likely based on dissociation equilibria.

Conclusion

Two new semi-bulky nitrogen-confused *C*-scorpionate ligands, $^{Ts}L^{iPr2}$ and $^{H}L^{iPr2}$, and their 1:1 and 1:2 M/L complexes of silver(I) and copper(I) have been prepared. In the solid state, the new C-scorpionate ligands bind silver(I) or copper(I) in similar fashion. The monoligated complexes 1a and 3a have κ^3N-ligands similar to that found in [Ag($^{Ts}L^*$)](OTf). The ligands in each [Cu($^xL^{iPr2}$)$_2$](PF$_6$) and [Ag($^xL^*$)$_2$](OTf) (x = Ts, H) coordinate the respective metals in similar κ^2N- modes by using the "normal" pyrazolyls, leaving the "confused" pyrazolyl unbound. In CH_3CN solution, all eight of the new metal complexes are involved in ligand dissociation and ligand redistribution equilibria that favor [M($^xL^{iPr2}$)(CH_3CN)$_n$]$^+$ at room temperature and above. These multiple equilibria distinguish the group 11 complexes of *C*-scorpionates from the complexes with boron-centered (normal) scorpionates that generally remain as monomeric single species in solution. Each of the new complexes was capable of catalyzing the aziridination of styrene at room temperature in CH_2Cl_2 using PhI=NTs as a nitrene transfer agent or in CH_3CN at 80 °C using in-situ formed PhI=NTs with the copper complexes generally being superior to their silver cousins. However, under the latter conditions, the extensive ligand dissociation in CH_3CN at 80 °C renders the ligand-free cuprous starting material, [Cu(CH_3CN)$_4$]PF$_6$, the superior catalyst. Under the former conditions, where dissociation is less extensive, the activity of the cationic [Cu($^xL^{iPr2}$)(CH_3CN)$_n$]$^+$ complexes appears, at least qualitatively, to be lower than that reported for charge neutral CuTp^x counterparts since yields of aziridine (obtained at room temperature) are lower than those reported for the latter. That is, it appears the reactivity of the group 11 scorpionate complexes increases inversely with their M^{2+}/M$^+$ redox couple, which is coarsely tuned by the charge of the scorpionate and more finely tuned by pyrazolyl substitutions. A detailed experimental and computational study of the relationship between electronic properties of group 11 scorpionates and aziridination activity is underway and will be reported on in due course.

Experimental Section

General Considerations:

The compound ^{Ts}pzC(O)H (Ts = *p*-SO$_2$C$_6$H$_4$CH$_3$) was prepared by the literature method.[39] PhI(OAc)$_2$, 3,5-diisopropylpyrazole or H(pz^{iPr2}), H$_2$NTs and styrene were purchased from commercial sources and used as received. Commercial anhydrous CoCl$_2$, AgOTf (OTf = trifluoromethanesulfonate), and [Cu(CH_3CN)$_4$]PF$_6$ were stored under argon in a drybox. Commercial solvents ethyl acetate (EtOAc), dichloromethane (DCM), methanol (MeOH) were used as received while diethyl ether (Et$_2$O), acetonitrile, toluene, and tetrahydrofuran (THF) were dried by conventional means and distilled under a nitrogen atmosphere prior to use. The silver(I) complexes were prepared under argon using Schlenk-

line techniques, however, after isolation, were stored and manipulated under normal laboratory atmospheric conditions, unless otherwise specified.

Instrumentation:

Melting point determinations were made on samples contained in glass capillaries using an Electrothermal 9100 apparatus and are uncorrected. ^{1}H (400 MHz), ^{13}C (101 MHz), ^{19}F (376 MHz), ^{31}P (162 MHz) NMR spectra were recorded on a Varian 400 MHz spectrometer. Chemical shifts were referenced to partly deuterated solvent resonances at δ_H = 7.26 and δ_C = 77.23 for CDCl$_3$ or δ_H = 1.94 and δ_C = 118.26 for CD$_3$CN. Abbreviations for NMR: br (broad), sh (shoulder), m (multiplet), ps (pseudo-), s (singlet), d (doublet), t (triplet), q (quartet), p (pentet), sept (septet), "confused" pyrazolyl = pz^{cf}, diisopropylpyrazolyl = pz$i$Pr. Electrochemical measurements were collected under a nitrogen atmosphere for samples as 0.1 mM solutions in CH$_3$CN with 0.1 M NBu$_4$PF$_6$ as the supporting electrolyte. A three-electrode cell comprised of an Ag/AgCl electrode (separated from the reaction medium with a semipermeable polymer membrane filter), a platinum working electrode, and a glassy carbon counter electrode was used for the voltammetric measurements. With this set up, the ferrocene/ferrocenium couple had an $E_{1/2}$ value of +0.44 V in CH$_3$CN at a scan rate of 200 mV/s, consistent with the literature values.[81] ESI(+) mass spectrometric measurements were obtained on a Micromass Q-TOF spectrometer where formic acid (ca. 0.1 % v:v) was added to the mobile phase (CH$_3$CN).

Ligand Syntheses

^{Ts}L^{iPr2}:

Method A. An argon-purged solution of 3,5-diisopropylpyrazole (4.57 g, 30.0 mmol) in 20 mL of THF was transferred slowly via cannula over 10 minutes to a suspension of NaH (0.75 g, 31.0 mmol) in 20 mL of THF under argon atmosphere. To ensure quantitative transfer, the flask originally containing 3,5-diisopropylpyrazole was rinsed with THF (2 × 5 mL) and the washings were transferred to the reaction mixture. After 10 minutes of stirring, thionyl chloride (1.1 mL, 15.0 mmol) was added by syringe slowly over 5 minutes; a colorless precipitate formed during the addition. The suspension was stirred at room temperature for 10 minutes, then CoCl$_2$ (0.065 g, 0.5 mmol) and ^{Ts}PzC(O)H (2.5 g, 10.0 mmol) were added sequentially as solids under an argon blanket. The blue suspension was heated at reflux under argon for 12 h, and then was cooled to room temperature. Solvent was removed by vacuum distillation and the solid residue was dissolved in 200 mL of a 1:1 biphasic mixture of H$_2$O:ethyl acetate. The organic layer was separated and the aqueous layer was extracted with dichloromethane (2 × 50 mL). The organic fractions were combined, dried with MgSO$_4$, and filtered. Solvents were removed by rotary evaporation to leave 6.02 g of crude product. The crude product was dissolved in 50 mL of boiling MeOH and the solution was stored at −10 °C for 1 h. The colorless crystalline product (4.5 g) was collected by vacuum filtration and was dried at room temperature under oil-pump vacuum. The mother liquor was concentrated to 10 mL and was stored at −10 °C for overnight to give another 0.3 g of pure product. The yield is 4.8 g (91 %).

Method B.
Under an argon atmosphere, a solution of 0.975 g (3.28 mmol) of triphosgene in 20 mL of THF was added dropwise to a solution of 3.00 g (19.7 mmol) of 3,5-diisopropylpyrazole and 2.75 mL (mmol) NEt$_3$ in 80 mL of THF. After stirring 16 h at 22 °C, the insoluble HNEt$_3$Cl was removed by filtration and

was washed with THF (2 × 10 mL). Solvent was removed from the combined THF fractions by vacuum distillation to leave a 95:5 mixture of (Pz^{iPr2})$_2$C=O:H(pz^{iPr2}) as a colorless oil that was used directly. ^{1}H NMR (CDCl$_3$): (Pz^{ipr})$_2$C=O: 6.12 (s, 2 H, H$_4$pz$i$Pr), 3.34 (sept, J = 6.8 Hz, 2 H, CHMe$_2$), 2.97 (sept, J = 6.9 Hz, 2 H, CHMe$_2$), 1.27 (d, J = 6.8 Hz, 12 H, iPr-CH$_3$), 1.24 (d, J = 6.9 Hz, 12 H, iPr-CH$_3$), H(pz^{iPr2}): 5.95 (s, 1 H, H$_4$pz$i$Pr), 3.03 (sept, J = 6.8 Hz, 2 H, CHMe$_2$), 1.34 (d, J = 6.8 Hz, 12 H, iPr-CH$_3$). Next, 2.15 g (9.85 mmol) ^{Ts}PzC(O)H, 0.0640 g (0.490 mmol) of CoCl$_2$ and 50 mL of toluene were added and the mixture was heated at reflux under argon for 16 h. Then, the resulting blue mixture was cooled to room temperature, and the solvent was removed by vacuum distillation. The residue was partitioned between 100 mL of H$_2$O and 100 mL of ethyl acetate. The layers were separated, and the aqueous layer was extracted with two 50 mL portions of CH$_2$Cl$_2$. The organic fractions were combined, dried with MgSO$_4$, and filtered. Solvents were removed by vacuum distillation to leave 4.04 g (76 %) of white solid. Recrystallization by cooling a boiling MeOH solution (50 mL) to −20 °C for 1 h and filtering gave 3.45 g (65 % yield) of pure ^{Ts}L^{iPr2} as colorless crystals after filtration and drying under vacuum. Mp: 140–143 °CC. ^{1}H NMR (CDCl$_3$): δ_H = 8.03 (d, J = 2.7 Hz, 1 H, H$_5$pz^{cf}), 7.81 (d, J = 8.3 Hz, 2 H, TsAr), 7.64 (s, 1 H, CH$_{methine}$), 7.26 (d, J = 8.3 Hz, 2 H, TsAr), 6.35 (d, J = 2.7 Hz, 1 H, H$_4$pz^{cf}), 5.85 (s, 2 H, H$_4$pz$i$Pr), 3.19 (sept, J = 6.9 Hz, 2 H, CHMe$_2$), 2.85 (sept, J = 6.9 Hz, 2 H, CHMe$_2$), 2.40 (s, 3 H, Ts-CH$_3$), 1.17 (d, J = 7.0 Hz, 12 H, iPr-CH$_3$), 0.95 (d, J = 6.8, 6 H, iPr-CH$_3$), 0.91 (d, J = 6.8, 6 H, iPr-CH$_3$). ^{1}H NMR (CD$_3$CN): δ_H = 8.19 (d, J = 2.7 Hz, 1 H, H$_5$pz^{cf}), 7.81 (d, J = 8.4 Hz, 2 H, TsAr), 7.62 (s, 1 H, H$_{meth}$), 7.49 (d, J = 8.4 Hz, 2 H, TsAr), 6.33 (d, J = 2.7 Hz, 1 H, H$_4$pz^{cf}), 5.98 (s, 2 H, H$_4$pz$i$Pr), 3.14 (sept, J = 6.8 Hz, 2 H, CHMe$_2$), 2.80 (sept, J = 6.9 Hz, 2 H, CHMe$_2$), 2.40 (s, 3 H, Ts-CH$_3$), 1.15 (d, J = 6.9 Hz, 12 H, iPr-CH$_3$), 0.98 (d, J = 6.8, 6 H, iPr-CH$_3$), 0.87 (d, J = 6.8, 6 H, iPr-CH$_3$). ^{13}C NMR (CDCl$_3$): δ_C = 158.47 (C$_5$pz$i$Pr), 145.99, 134.34, 131.89, 130.00, 128.51, 109.82 (C$_4$pz$i$Pr), 100.20 (C$_4$pz^{cf}), 69.99 (C$_{meth}$), 28.00, 25.52, 23.73, 23.02, 22.98, 22.83, 21.88 (Ts-CH$_3$).

^{H}L^{iPr2}:

A solution of 20.0 mL of 5.00 M NaOH (aq) (100.0 mmol), 3.50 g (6.52 mmol) ^{Ts}L^{iPr2}, and 20 mL of THF was heated at reflux for 20 min until completion (as monitored by ^{1}H NMR and/or TLC). After the mixture had cooled to room temperature, the THF layer was separated and the aqueous layer was extracted with dichloromethane (2 × 20 mL). The combined organic fractions were dried with MgSO$_4$ and filtered. The organic solvents were removed by vacuum distillation to leave 2.42 g (97 %) of pure ^{H}L^{iPr2} as a white solid. Mp: 137–138 °CC. ^{1}H NMR (CDCl$_3$): δ_H = 7.83 (s, 1 H), 7.50 (d, J = 2.0 Hz, 1 H, H$_4$pz^{cf}), 6.22 (d, J = 2.0 Hz, 1 H, H$_4$pz^{cf}), 5.89 (s, 2 H, H$_4$pz$i$Pr), 3.34 (sept, J = 6.8 Hz, 2 H, CHMe$_2$), 2.92 (sept, J = 6.9 Hz, 2 H, CHMe$_2$), 1.23 (d, J = 6.9 Hz, 12 H, iPr-CH$_3$), 1.02 (d, J = 6.8 Hz, 6 H, iPr-CH$_3$), 0.93 (d, J = 6.8 Hz, 6 H, iPr-CH$_3$); N-H not observed. ^{1}H NMR (CD$_3$CN): δ_H = 11.12 (br, s, 1 H, NH), 7.72 (s, 1 H, H$_{meth}$), 7.56 (d, J = 2.2 Hz, 1 H, H$_5$pz^{cf}), 6.11 (d, J = 2.2 Hz, 1 H, H$_4$pz^{cf}), 6.00 (s, 2 H, H$_4$pz^{iPr2}), 3.33 (sept, J = 6.9 Hz, 2 H, CHMe$_2$), 2.85 (sept, J = 6.9 Hz, 2 H, CHMe$_2$), 1.19 (d, J = 6.9 Hz, 12 H, iPr-CH$_3$), 1.07 (d, J = 6.8 Hz, 6 H, iPr-CH$_3$), 1.00 (d, J = 6.8 Hz, 6 H, iPr-CH$_3$). ^{13}C NMR (CDCl$_3$): δ_C = 158.72 (C$_5$pz^{cf}), 152.37, 142.88, 135.36, 105.88 (C$_4$pz^{cf}), 100.45 (C$_4$pz$i$Pr), 69.61 (C$_{meth}$), 28.06 (CHMe$_2$), 25.34 (CHMe$_2$), 23.86 (iPr-CH$_3$), 23.05 (iPr-CH$_3$), 23.02 (iPr-CH$_3$), 22.85 (iPr-CH$_3$).

Metal Complex Syntheses

General Procedure. A:

Under argon, the desired ligand (1 or two equivalents) and either AgOTf or [Cu(CH$_3$CN)$_4$]PF$_6$ were dissolved in 10 mL of CH$_3$CN and stirred 3 h at room temperature. Solvent was removed under vacuum

and the residue was washed with 2 mL of Et$_2$O (or if too soluble, like 1b or 3b, 2 mL of hexane), filtered, and the precipitate was dried under vacuum at 60 °C 2 h.

General Procedure. B:

A solution of a given ligand (1 or 2 equiv.) in 10 mL of THF was added to a solution of AgOTf in 10 mL of THF by cannula transfer. The flask originally containing the ligand was washed twice with 2 mL of THF, and the washings were transferred to the reaction medium to ensure quantitative transfer of the reagent. After the mixture has been stirred for 2 h, the solvent was removed by vacuum distillation. The colorless residue was washed with two 2 mL portions of Et$_2$O and was dried under vacuum for an hour. The quantities of the reagents used and of the products obtained and characterization data for each of the four new compounds are given below. An alternative workup in the case where a precipitate was observed is also described.

[Ag(^{Ts}L^{iPr2})](OTf), 1a:

Using General Procedure A, a mixture of 0.300 g (0.559 mmol) of ^{Ts}L^{iPr2} and 0.140 g (0.559 mmol) of AgOTf gave 0.417 g (94 %) of 1a as a colorless solid. Using General procedure B, a mixture of 0.502 g (0.935 mmol) of ^{Ts}L^{iPr2} and 0.240 g (0.935 mmol) of AgOTf gave 0.609 g (82 %) of 1a as a colorless solid. Mp: 180–182 °CC. Anal. Calcd (found) for C$_{30}$H$_{40}$AgF$_3$N$_6$O$_5$S$_2$: C, 45.40 (45.43), H, 5.08 (4.95), N, 10.59 (10.70). ^{1}H NMR (CD$_3$CN): δ_H = 8.20 (d, J = 2.7 Hz, 1 H, H$_5$pz^{cf}), 7.75 (d, J = 8.4 Hz, 2 H, TsAr), 7.51 (s, 1 H, H$_{methine}$), 7.39 (d, J = 8.4 Hz, 2 H, TsAr), 6.19 (s, 2 H, H$_4$pz$i$Pr), 6.02 (br s, 1 H, H$_4$pz^{cf}), 3.18 (sept, J = 6.7 Hz, 2 H, CHMe$_2$), 2.73 (br m, 2 H, CHMe$_2$), 2.40 (s, 3 H, Ts-CH$_3$), 1.20 (d, J = 6.8 Hz, 6 H, iPr-CH$_3$), 1.17 (d, J = 6.7 Hz, 6 H, iPr-CH$_3$), 1.12 (br s, 12 H, iPr-CH$_3$). ^{13}C NMR (CD$_3$CN): δ_C = 162.46, 154.91, 154.69, 147.93, 134.32, 133.96, 131.22, 128.89, 122.16 (q, J = 321 Hz, CF$_3$), 110.02, 100.76, 64.61, 29.36, 26.47, 23.54, 22.96, 22.27, 21.71. ^{19}F NMR (CD$_3$CN): –79.33 ppm. ESI(+) MS, m/z (rel. abund. %) [assignment]: ESI(+) MS, m/z (rel. abund. %) [assignment]: 1182 (38) [Ag(L)$_2$]$^+$, 645 (100) [Ag(L)]$^+$, 537 (78) [H(L)]$^+$, 385 (10) [L – pz^{iPr2}]$^+$. Crystal of 1a·acetone suitable for single-crystal X-ray diffraction were obtained by layering hexanes over a solution of 50 mg of 1a in 2 mL of acetone and allowing solvents to slowly diffuse over 16 h.

[Ag(^{Ts}L^{iPr2})$_2$](OTf), 1b:

Using General Procedure A, a mixture of 0.500 g (0.935 mmol) of ^{Ts}L^{iPr2} and 0.120 g (0.468 mmol) of AgOTf gave 0.620 g (90 %) of 1b as a colorless solid. By adopting a modification of General Procedure B, a mixture of 0.506 g (0.943 mmol) of ^{Ts}L^{iPr2} and 0.121 g (0.472 mmol) of AgOTf gave a colorless precipitate immediately. Filtration and drying the precipitate under vacuum (no washing) gave 0.530 g (84 %) 1b as a colorless solid. On the other hand, if the general procedure is strictly followed (in a separate experiment of the same scale), where the colorless precipitate was collected by cannula filtration after 2 h, and the insoluble portion is washed with two 2 mL portions of Et$_2$O and dried under vacuum for an hour, then 0.353 g (56 %) of 1b is obtained a colorless solid. An additional 0.158 g (25 %) of 1b (81 % total yield) can be recovered from the THF soluble portion by removing solvent, washing the residue with 1 mL of Et$_2$O, and drying under vacuum. Mp: 128–130 °CC. Anal. Calcd (found) for C$_{59}$H$_{80}$AgF$_3$N$_{12}$O$_7$S$_3$: C, 53.27 (53.49), H, 6.06 (6.20), N 12.63 (12.39). ^{1}H NMR (CD$_3$CN): δ_H = 8.18 (d, J = 2.8 Hz, 1 H, H$_5$pz^{cf}), 7.75 (d, J = 8.3 Hz, 2 H, TsAr), 7.53 (s, 1 H, CH$_{meth}$), 7.38 (d, J = 8.3 Hz, 2 H, TsAr), 6.11 (s, 2 H, H$_4$pz$i$Pr), 6.01 (br s, 1 H, H$_4$pz^{cf}), 3.18 (sept, J = 6.7 Hz, 2 H, CHMe$_2$), 2.45 (br s, 2 H, CHMe$_2$), 2.40 (s, 3 H, Ts-CH$_3$), 1.12 (d, J = 6.7 Hz, 12 H, iPr-CH$_3$), 0.95 (br s, 12 H, iPr-CH$_3$). ^{13}C NMR (CD$_3$CN): 162.26 (br s), 155.32, 154.95 (br s), 147.86, 134.43, 133.62, 131.21, 128.91, 122.17 (q, J = 321 Hz, CF$_3$),

109.88 (C$_4$pz^{cf}), 100.78 (C$_4$pz$i$Pr), 65.76 (C$_{meth}$), 29.10 (br s), 26.47, 23.74, 23.36, 23.28, 21.89 (br s), 21.69. ^{19}F NMR (CD$_3$CN): −79.34 ppm. ESI(+) MS, *m/z* (rel. abund. %) [assignment]: 1182 (33) [Ag(L)$_2$]$^+$, 645 (11) [Ag(L)]$^+$, 537 (100) [H(L)]$^+$, 385 (37) [L − pz^{iPr2}]$^+$.

[Ag(^{H}L^{iPr2})](OTf), 2a:
Using General Procedure A, a mixture of 0.427 g (1.12 mmol) of ^{H}L^{iPr2} and 0.287 g (1.12 mmol) of AgOTf gave 0.647 g (94 %) of 2a as a colorless solid. By using General Procedure B, a mixture of 0.510 g (1.33 mmol) of ^{H}L^{iPr2} and 0.343 g (1.33 mmol) of AgOTf gave 0.729 g (86 %) of 2a as a colorless solid. Mp: 113–115 °CC. Anal. Calcd (found) for C$_{23}$H$_{34}$N$_6$SO$_3$F$_3$Ag: C, 43.30 (42.99), H, 5.35 (5.36), N 13.14 (12.87). ^{1}H NMR (CD$_3$CN): δ_H = 7.66 (d, *J* = 2.5 Hz, 1 H, H$_5$pz^{cf}), 7.60 (s, 1 H, CH$_{methine}$), 6.25 (br s, 1 H, H$_4$pz^{cf}), 6.16 (s, 2 H, H$_4$pz$i$Pr), 3.30 (sept, *J* = 6.7 Hz, 2 H, CHMe$_2$), 2.86 (sept, *J* = 6.9 Hz, 2 H, CHMe$_2$), 2.39 (br s, 1 H, N-H), 1.24 (d, *J* = 6.9 Hz, 12 H, iPr-CH$_3$), 1.18 (d, *J* = 6.7 Hz, 12 H, iPr-CH$_3$). ^{13}C NMR (CD$_3$CN): δ_C = 161.45, 153.81, 105.99, 100.54, 64.01, 29.34, 26.43, 23.81, 23.20, 22.90, 22.78, 22.67, CF$_3$ not observed. ^{19}F NMR (CD$_3$CN): −79.34 ppm. ESI(+) MS, *m/z* (rel. abund. %) [assignment]: 872 (100) [Ag(L)$_2$]$^+$, 530 (12) [Ag(L)(CH$_3$CN)]$^+$, 489 (67) [Ag(L)]$^+$, 383 (8) [H(L)]$^+$, 231 (6) [L − pz^{iPr2}]$^+$, 190 (2) [Ag(CH$_3$CN)$_2$]$^+$, 153 (7) [H$_2$pz^{iPr2}]$^+$.

[Ag(^{H}L^{iPr2})$_2$](OTf), 2b:
Using General Procedure A, a mixture of 0.300 g (0.784 mmol) of ^{H}L^{iPr2} and 0.101 g (0.392 mmol) of AgOTf gave 0.374 g (90 %) of 2b as a colorless solid. By using General Procedure B, a mixture of 0.524 g of (1.37 mmol) of ^{H}L^{iPr2} and 0.176 g (1.37 mmol) of AgOTf gave 0.559 g (80 %) of 2b as a colorless solid after drying under vacuum for an hour. Mp: 125–127 °CC. Anal. Calcd (found) for C$_{45}$H$_{68}$N$_{12}$SO$_3$F$_3$Ag: C, 52.88 (52.89), H, 6.70 (6.67), N 16.44 (16.35). ^{1}H NMR (CD$_3$CN, 293 K): 11.23 (br s, 2 H, NH), 7.63 (s, 2 H, CH$_{meth}$), 7.60 (d, *J* = 2.1 Hz, 2 H, H$_5$pz^{cf}), 6.14 (d, *J* = 2.1 Hz, 2 H, H$_4$pz^{cf}), 6.09 (s, 4 H, H$_4$pz$i$Pr), 3.30 (sept, *J* = 6.8 Hz, 4 H, CHMe$_2$), 2.46 (br sept, *J* = 6.7 Hz, 4 H, CHMe$_2$) 1.20 (d, *J* = 6.8 Hz, 12 H, iPr-CH$_3$), 1.20 (d, *J* = 6.8 Hz, 12 H, iPr-CH$_3$), 1.00 (d, *J* = 6.7 Hz, 12 H, iPr-CH$_3$), 0.99 (d, *J* = 6.7 Hz, 12 H, iPr-CH$_3$). ^{13}C NMR (CD$_3$CN): δ_C = 161.80, 154.25, 148.41, 131.04, 122.11 (q, *J* = 324 Hz, CF$_3$), 105.68 (C4pz^{cf}), 100.45 (C4pz$i$Pr), 64.95 (C$_{meth}$), 29.20, 26.52, 25.48, 23.66, 23.60, 23.06, 22.24. ^{19}F NMR (CD$_3$CN): −79.34 ppm. ESI(+) MS, *m/z* (rel. abund. %) [assignment]: 872 (100) [Ag(L)$_2$]$^+$, 530 (3) [Ag(L)(CH$_3$CN)]$^+$, 489 (28) [Ag(L)]$^+$, 383 (92) [H(L)]$^+$, 231 (79) [L pz^{iPr2}]$^+$, 153 (6) [H$_2$pz^{iPr2}]$^+$.

[Cu(^{Ts}L^{iPr2})(CH$_3$CN)](PF$_6$), 3a:
Using General Procedure A, a mixture of 0.500 g of (0.935 mmol) of ^{Ts}L^{iPr2} and 0.347 g (0.935 mmol) of [Cu(CH$_3$CN)$_4$]PF$_6$ gave 0.655 g (89 %) of 3a as a pale yellow powder after drying at 60 °C under vacuum for an hour. Anal. Calcd (found) for C$_{31}$H$_{43}$N$_7$CuF$_6$O$_2$PS: C, 47.18 (46.86), H, 5.49 (5.36), N 12.42 (12.77). Mp: 95–97 °CC. The NMR spectra have signals for an equilibrium mixture of 3a, 3b, ^{Ts}L^{iPr2}, and [Cu(CH$_3$CN)$_4$]PF$_6$ with relative compositions that are both temperature and concentration dependent (vide infra), only those resonances for 3a are reported below. ^{1}H NMR (CD$_3$CN): δ_H = 8.15 (d, *J* = 2.7 Hz, 1 H, H$_5$pz^{cf}), 7.76 (d, *J* = 8.3 Hz, 2 H, TsAr), 7.41 (s, 1 H, CH$_{meth}$) 7.38 (d, *J* = 8.3 Hz, 2 H, TsAr), 6.21 (s, 2 H, H$_4$pz$i$Pr), 5.91 (br m, 1 H, H$_4$pz^{cf}), 3.18 (sept, *J* = 6.8 Hz, 2 H, CHMe$_2$), 3.05 (br m, 2 H, CHMe$_2$), 2.41 (s, 3 H, Ts-CH$_3$), 1.23 (d, *J* = 6.8 Hz, 12 H, iPr-CH$_3$), 1.20 (d, *J* = 6.8 Hz, 12 H, iPr-CH$_3$). ^{13}C NMR (CD$_3$CN): δ_C = 162.19, 154.80, 154.24, 148.00, 134.24, 133.71, 131.19, 128.94, 109.53 (C$_4$pz$i$Pr), 100.53 (C$_4$-pz^{cf}), 64.22 (C$_{methine}$), 28.96, 26.36, 23.63, 23.27, 22.85, 22.40, 21.70. ^{31}P NMR (CD$_3$CN): δ_p -144.64 (sept, *J*$_{PF}$ = 706 Hz). ^{19}F NMR (CD$_3$CN) δ_F = -72.93 (d, *J*$_{FP}$ = 706 Hz). ESI(+) MS, *m/z* (rel. abund. %) [assignment]: 1136 (15) [Cu(L)$_2$]$^+$, 640 (80) [Cu(L)(CH$_3$CN)]$^+$, 599 (100) [Cu(L)]$^+$, 537 (97) [H(L)]$^+$, 385 (73) [L pz^{iPr2}]$^+$.

Crystals suitable for X-ray diffraction were grown by layering 4 mL of hexane onto a solution of 50 mg of 3a in 1 mL of CH_2Cl_2 and allowing solvents to diffuse 14 h.

[Cu($^{Ts}L^{iPr2}$)$_2$](PF$_6$), 3b:

Using General Procedure A, a mixture of 0.100 g of (0.186 mmol) of $^{Ts}L^{iPr2}$ and 0.0347 g (0.093 mmol) of [Cu(CH$_3$CN)$_4$]PF$_6$ gave 0.116 g (86 %) of 3b as a colorless powder after drying under vacuum for an hour. Anal. Calcd (found) for $C_{58}H_{80}F_6N_{12}O_4PS_2Cu$: C, 54.34 (54.46), H, 6.29 (6.27), N 13.11 (13.44). Mp: 90–92 °CC. The NMR spectra have signals for an equilibrium mixture of 3b, 3a, $^{Ts}L^{iPr2}$, and [Cu(CH$_3$CN)$_4$]PF$_6$ with relative compositions that are both temperature and concentration dependent (vide infra), only those resonances for 3b are reported below. ^{1}H NMR (CD$_3$CN, 295 K): δ_H = 8.13 (d, J = 1.3 Hz, 2 H, H$_5$pz^{cf}), 7.76 (d, J = 7 Hz, 4 H, TsAr), 7.41 (s, 2 H, CH$_{meth}$), 7.35 (d, J = 7 Hz, 4 H, TsAr), 6.21 (s, 2 H, H$_4$pziPr), 6.08 (s, 2 H, H$_4$pziPr), 5.45 (d, 2 H, H$_4$pz^{cf}), 3.16 (sept, J = 6 Hz, 2 H, CHMe$_2$), 3.04 (m, 1 H, CHMe$_2$), 2.38 (d, 6 H, Ts-Me), 2.26 (m, 1 H, CHMe$_2$), 1.26–1.18 (m, 24 H, iPr-Me), 0.84 (d, J = 6.6 Hz, 6 H, iPr-Me), 0.80 (d, J = 6.6 Hz, 6 H, iPr-Me), 0.55 (dd, J = 6.5 Hz, 6 H, iPr-Me), 0.43 (dd, J = 6.5 Hz, 6 H). ^{31}P NMR (CD$_3$CN): δ_p -144.64 (sept, J_{PF} = 706 Hz). ^{19}F NMR (CD$_3$CN) δ_F = -72.93 (d, J_{FP} = 706 Hz). ESI(+) MS, m/z (rel. abund. %) [assignment]: 1136 (9) [Cu(L)$_2$]$^+$, 640 (95) [Cu(L)(CH$_3$CN)]$^+$, 599 (100) [Cu(L)]$^+$, 537 (35) [H(L)]$^+$, 385 (26) [L–pz^{iPr2}]$^+$, 145 (2) [Cu(CH$_3$CN)$_2$]$^+$. Crystals of 3b·CH$_2$Cl$_2$ suitable for single-crystal X-ray diffraction were obtained by layering hexanes over a solution of 30 mg of 3b in 1 mL of dichloromethane and allowing solvents to slowly diffuse over 16 h.

[Cu($^{H}L^{iPr2}$)(CH$_3$CN)](PF$_6$), 4a:

Using General Procedure A, a mixture of 0.300 g of (0.784 mmol) of $^{H}L^{iPr2}$ and 0.292 g (0.784 mmol) of [Cu(CH$_3$CN)$_4$]PF$_6$ gave 0.480 g (97 %) of 4a·CH$_3$CN as an off-white powder after drying at 60 °C under vacuum for an hour. Anal. Calcd (found) for $C_{24}H_{37}N_7CuF_6P$: C, 45.61 (45.99), H, 5.90 (5.83), N 15.51 (15.14). Mp: 157–159 °CC. The NMR spectra have signals for an equilibrium mixture of 4a, 4b, $^{H}L^{iPr2}$, and [Cu(CH$_3$CN)$_4$]PF$_6$ with relative compositions that are both temperature and concentration dependent (vide infra), only those resonances for 4a are reported below. ^{1}H NMR (CD$_3$CN, 293 K): 11.64 (br s, 1 H, NH), 7.66 (br d, J = 1 Hz, 1 H, H$_5$-pz^{cf}), 7.48 (s, 1 H, H$_{meth}$), 6.46 (br d, J = 1 Hz, 1 H, H$_4$-pz^{cf}), 6.12 (s, 2 H, H$_4$-pziPr), 3.31 (sept, J = 6.7 Hz, 2 H, CHMe$_2$), 3.06 (br sept, J = 6.6 Hz, 2 H, CHMe$_2$), 1.28 (d, J = 6.7 Hz, 6 H, CH$_3$), 1.25–1.21 (br m, 18 H, CH$_3$). ^{13}C NMR (CD$_3$CN, 293 K): δ_C = 161.18 (C$_{3/5}$-pziPr), 152.92 (C$_{3/5}$-pziPr), 147.20 (C$_{3/5}$-pz^{cf}), 130.91 (C$_{3/5}$-pz^{cf}), 105.43 (C$_4$-pz^{cf}), 100.40 (C$_4$-pziPr), 62.53 (C$_{meth}$), 28.92 (CHMe$_2$), 26.29 (CHMe$_2$), 24.08 (CH$_3$), 22.93 (CH$_3$), 22.76 (CH$_3$), 22.49 (CH$_3$). ^{31}P NMR (CD$_3$CN): δ_p -144.63 (sept, J_{PF} = 707 Hz). ^{19}F NMR (CD$_3$CN) δ_F = -72.93 (d, J_{FP} = 707 Hz). ESI(+) MS, m/z (rel. abund. %) [assignment]: 827 (1) [Cu(L)$_2$]$^+$, 676 (1) [Cu(L)(L – pz^{iPr2})]$^+$, 486 (100) [Cu(L)(CH$_3$CN)]$^+$, 445 (12) [Cu(L)]$^+$, 383 (5) [H(L)]$^+$, 231 (5) [L – pz^{iPr2}], 145 (5) [Cu(CH$_3$CN)$_2$]$^+$.

[Cu($^{H}L^{iPr2}$)$_2$](PF$_6$), 4b:

Using General Procedure A, a mixture of 0.300 g of (0.784 mmol) of $^{H}L^{iPr2}$ and 0.146 g (0.392 mmol) of [Cu(CH$_3$CN)$_4$]PF$_6$ gave 0.420 g (94 %) of 4b as colorless powder after drying under vacuum for an hour. Anal. Calcd (found) for $C_{44}H_{68}N_{12}CuF_6P$: C, 54.28 (54.33), H, 7.04 (6.72), N 17.26 (17.07). Mp: 132–134 °CC. The NMR spectra have signals for an equilibrium mixture of 4a, 4b, $^{H}L^{iPr2}$, and [Cu(CH$_3$CN)$_4$]PF$_6$ with relative compositions that are both temperature and concentration dependent (vide infra), only those resonances for 4b are reported below. ^{1}H NMR (CD$_3$CN, 293 K): 11.18 (br s, 2 H, NH), 7.59 (br s, 2 H, H$_5$pz^{cf}), 7.53 (s, 2 H, CH$_{meth}$), 6.35 (br s, H$_4$pz^{cf}), 6.15 (s, H$_4$pziPr), 6.09 (s, H$_4$pziPr), 5.29 (br s, H$_4$pz^{cf}), 3.29 (sept, J = 6.8 Hz, 4 H, CHMe$_2$), 2.97 (br m, 2 H, CHMe$_2$), 2.18 (br m, 2 H, CHMe$_2$), 1.34 –1.09 (br m, 24

H, *i*Pr-CH$_3$), 0.89 (br s, 12 H, *i*Pr-CH$_3$), 0.59 (br s, 6 H, *i*Pr-CH$_3$), 0.45 (br s, 6 H, *i*Pr-CH$_3$), see text for explanation. ^{31}P NMR (CD$_3$CN): δ_P -144.65 (sept, J_{PF} = 707 Hz). ^{19}F NMR (CD$_3$CN) δ_F = -72.92 (d, J_{FP} = 707 Hz). ESI(+) MS, *m/z* (rel. abund. %) [assignment]: 827 (50) [Cu(L)$_2$]$^+$, 486 (100) [Cu(L)(CH$_3$CN)]$^+$, 445 (29) [Cu(L)]$^+$, 383 (30) [H(L)]$^+$, 231 (60) [L − pz^{iPr2}]. Crystals of 4b·2THF were grown under an Ar atmosphere in the drybox by layering 5 mL of hexanes onto a solution of 30 mg of 4b in 1 mL of THF and allowing solvents to diffuse over 12 h.

Catalytic Aziridination

For most consistent results that minimize uncertainties in weighing small masses of solid catalysts, 0.05 M stock solutions of complexes, or separate 0.05 M solutions of ligands and metals were prepared and used in catalysis reactions.

General Procedure. Method A:

In an argon-filled drybox, a 20 mL vial was charged with 0.5 g of activated 4 Å molecular sieves and 0.20 mL of a 0.05 M stock solution of pre-formed metal catalyst (0.010 mmol, 0.02 equiv.). Alternatively, for in-situ formed catalysts 0.2 mL of a 0.05 M solution of either AgOTf or [Cu(CH$_3$CN)]PF$_6$ in CH$_2$Cl$_2$ and either a 0.2 mL or a 0.4 mL of CH$_2$Cl$_2$ solution that is 0.05 M in ^{X}L^R (for 1:1 and 1:2 M/^{X}L^R complexes, 0.01 mmol, 0.02 equiv.) was added. Then, CH$_2$Cl$_2$ was added to give a total volume of 5 mL. The mixture was stirred for 5 min to generate the metal catalyst, then 0.215 g (0.575 mmol, 1.15 equiv.) of PhINTs and 57 µL (0.5 mmol, 1.0 equiv.) of styrene were added. After the mixture had been stirred for 24 h at room temperature, it was filtered through a 2 cm silica pad and 3 mL of CH$_2$Cl$_2$ was used to rinse the silica pad. Next, 11.1 mg (0.05 mmol) of 1,4-bis(trimethylsilyl)benzene was added to the filtrate as an NMR standard, and the solvent was removed under vacuum at room temperature to leave a brown-orange oily residue. This NMR standard is relatively nonvolatile under most mild conditions (rotary evaporator at house vacuum of 1 Torr); however, this compound will partly sublime if heated at 70 °C under oil pump vacuum (10^{-4} Torr) for several hours, so care should be taken to avoid extended heating under modest to high vacuum. NMR yields of *N*-tosyl-2-phenylaziridine (conversion % with respect to *N*-tosylamine) in the brown-orange oily residue dissolved in CDCl$_3$ were obtained by relative integrations as follows. First the singlet resonance at δ_H = 0.26 ppm for SiCH$_3$ hydrogens was set to 18 H. Next the average integration value for the resonances at δ_H = 3.78 (dd, *J* = 7.2, 4.6 Hz, 1 H) and δ_H = 2.98 (d, *J* = 7.2 Hz, 1 H) for aziridinyl ring hydrogens was taken (the third doublet resonance is obscured by the tosyl methyl resonance near 2.4 ppm). The average integration value is then multiplied by the known µmol of C$_6$H$_4$(SiMe$_3$)$_2$ and 100 % to give the % conversion to aziridine based on *N*-tosylamine. The average values of three independent runs are collected in Table **3**. The cited turnover numbers (TON) in the main text are calculated as the ratio of mmol aziridine to mmol catalyst.

Method B:

A 1.00 g sample of activated 4 Å molecular sieves and a Teflon-coated magnetic stir bar were added to a Schlenk flask under an argon blanket. The flask was flame-dried under vacuum, then was backfilled with argon, and cooled to room temperature. Next, either 0.4 mL of a 0.05 M stock solution of pre-formed metal catalyst (0.02 mmol, 0.02 equiv.) or separate CH$_3$CN solutions of metal salt (0.4 mL, 0.05 M, 0.02 equiv.) and ligand (0.4 mL of 0.05 M for monoligated complexes, or 0.8 mL of 0.05 M for diligated complexes), then enough CH$_3$CN was added to give a total volume of 4 mL. After the mixture

had been stirred five min, 0.171 g (1.00 mmol) of tosylamine, and 0.322 g (1.00 mmol) of PhI(OAc)$_2$ were added sequentially under an argon blanket giving either a colorless (silver catalysts) or blue (copper catalysts) solution. The reaction flask was placed in an oil bath maintained at 80 °C and allowed to equilibrate for 15 min. Then, 0.57 mL (0.52 g, 5.0 mmol) of styrene was added by syringe, at which time the solution changed color to either orange, or in some instances, orange-brown (for silver catalysts) or remained blue (for copper catalysts). After the reaction mixture had been stirred at 80 °C for 16 h, it was filtered through a sintered glass frit. The solid residue was washed with two 2 mL portions of CH$_3$CN. Next, between 20 and 30 mg (89.9 to 135 μmol) of 1,4-bis(trimethylsilyl)benzene was added to the filtrate as a nonvolatile NMR standard, and the solvent was removed by rotary evaporation (1 Torr, 40 °C) to leave a brown-orange oily residue that was subject to NMR analysis as above. A summary of results (average values of at least three independent runs) is collected in Table **4**.

X-ray Crystallography

X-ray intensity data from a colorless plate of 1a·acetone, a colorless block of 3a, a colorless prism of 3b·CH$_2$Cl$_2$, and a colorless plate of 4b·2THF were collected at 100.0(1) K with an Oxford Diffraction Ltd. Supernova equipped with a 135 mm Atlas CCD detector using Cu-K_α radiation, λ = 1.54184 Å. Raw data frame integration and Lp corrections were performed with CrysAlis Pro (Oxford Diffraction, Ltd.).**82** Final unit cell parameters were determined by least-squares refinement of 22190, 17870, 29178, and 7422 reflections from the data sets of 1a·acetone, 3a, 3b·CH$_2$Cl$_2$, and 4b·2THF, respectively, each with $I > 2\sigma(I)$. Analysis of the data showed negligible crystal decay during collection in each case. Direct methods structure solutions were performed with Olex2.solve**83** while difference Fourier calculations and full-matrix least-squares refinements against F2 were performed with SHELXTL.**84** Empirical (Gaussian) absorption corrections were applied using spherical harmonics implemented in the SCALE3 ABSPACK scaling algorithm. Hydrogen atoms were placed in idealized positions and included as riding atoms. For 1a·acetone, one of the isopropyl groups is unevenly (63:37 %) disordered over two nearby positions, affecting C14 (C14a) and C16 (C16a). For 3a·CH$_3$CN, the structure includes cavities apparently partially populated by disordered water molecules (ca. 30 %). Their contribution was accounted for by using a solvent-mask procedure SQUEEZE. Similarly, the structure of 4b·2THF had large cavities (1097.1 Å^3) populated with severely disordered THF solvent molecules, that were accounted for by using the SQEEZE procedure. A summary of crystal data and structure refinement is given in Tables S1 and S2.

CCDC 1985192 (for 1a·acetone), 1985193 (for 3a), 1985194 (for 3b·CH$_2$Cl$_2$), and 1985195 (for 4b·2THF) contain the supplementary crystallographic data for this paper. These data can be obtained free of charge from **The Cambridge Crystallographic Data Centre**.

Acknowledgements

Filename	Description
ejic202000173-sup-0001-SupMat.pdf2 MB	Supporting Information

Please note: The publisher is not responsible for the content or functionality of any supporting information supplied by the authors. Any queries (other than missing content) should be directed to the corresponding author for the article.

References

1 Y. Zhu, Q. Wang, R. G. Cornwall and Y. Shi, *Chem. Rev*, 2014, **114**, 8199– 8256.

2 G. Dequirez, V. Pons and P. Dauban, *Angew. Chem. Int. Ed*, 2012, **51**, 7384– 7395; *Angew. Chem*, 2012, **124**, 7498.

3 N. W. Goldberg, A. M. Knight, R. K. Zhang and F. H. Arnold, *J. Am. Chem. Soc.* 2019, DOI https://doi.org/10.1021/jacs.9b11608.

4 G. Storch, N. van den Heuvel and S. J. Miller, *Adv. Synth. Catal.* 2019, adsc.201900631.

5 B. Darses, R. Rodrigues, L. Neuville, M. Mazurais and P. Dauban, *Chem. Commun*, 2017, **53**, 493– 508.

6 C. Damiano, D. Intrieri and E. Gallo, *Inorg. Chim. Acta*, 2018, **470**, 51– 67.

7 S. Liang and M. P. Jensen, *Organometallics*, 2012, **31**, 8055– 8058.

8 A. Caballero, M. M. Díaz-Requejo, M. R. Fructos, J. Urbano, P. J. Pérez, in: *Ligand Design in Metal Chemistry*, John Wiley & Sons, Ltd, 2016, pp. 308– 329.

9 A. Fingerhut, O. V. Serdyuk and S. B. Tsogoeva, *Green Chem*, 2015, **17**, 2042– 2058.

10 V. Bagchi, P. Paraskevopoulou, P. Das, L. Chi, Q. Wang, A. Choudhury, J. S. Mathieson, L. Cronin, D. B. Pardue, T. R. Cundari, et al., *J. Am. Chem. Soc*, 2014, **136**, 11362– 11381.

11 F. Yang, J. Ruan, P. Y. Zavalij and A. N. Vedernikov, *Inorg. Chem*, 2019, **58**, 15562– 15572.

12 T. Corona, L. Ribas, M. Rovira, E. R. Farquhar, X. Ribas, K. Ray and A. Company, *Angew. Chem. Int. Ed*, 2016, **55**, 14005– 14008; *Angew. Chem*, 2016, **128**, 14211.

13 D. A. Evans, M. T. Bilodeau and M. M. Faul, *J. Am. Chem. Soc*, 1994, **116**, 2742– 2753.

14 P. J. Perez, M. Brookhart and J. L. Templeton, *Organometallics*, 1993, **12**, 261– 262.

15 M. A. Mairena, M. M. Díaz-Requejo, T. R. Belderraín, M. C. Nicasio, S. Trofimenko and P. J. Pérez, *Organometallics*, 2004, **23**, 253– 256.

16 L. Maestre, W. M. C. Sameera, M. M. Díaz-Requejo, F. Maseras and P. J. Pérez, *J. Am. Chem. Soc*, 2013, **135**, 1338– 1348.

17 M. M. Díaz-Requejo, P. J. Pérez, M. Brookhart and J. L. Templeton, *Organometallics*, 1997, **16**, 4399– 4402.

18 J. Moegling, A. Hoffmann, F. Thomas, N. Orth, P. Liebhäuser, U. Herber, R. Rampmaier, J. Stanek, G. Fink, I. Ivanović-Burmazović, et al., *Angew. Chem. Int. Ed*, 2018, **57**, 9154– 9159; *Angew. Chem*, 2018, **130**, 9294.

19 T. L. Lam, K. C.-H. Tso, B. Cao, C. Yang, D. Chen, X.-Y. Chang, J.-S. Huang and C.-M. Che, *Inorg. Chem*, 2017, **56**, 4253– 4257.

20 C. L. Mak, B. C. Bostick, N. M. Yassin and M. G. Campbell, *Inorg. Chem*, 2018, **57**, 5720– 5722.

21 R. J. Scamp, J. W. Rigoli and J. M. Schomaker, *Pure Appl. Chem*, 2014, **86**, 381– 393.

22 Z. Li and C. He, *Eur. J. Inorg. Chem*, 2006, **2006**, 4313– 4322.

23 M. Huang, J. R. Corbin, N. S. Dolan, C. G. Fry, A. I. Vinokur, I. A. Guzei and J. M. Schomaker, *Inorg. Chem*, 2017, **56**, 6725– 6733.

24 J. M. Alderson, J. R. Corbin and J. M. Schomaker, *Acc. Chem. Res*, 2017, **50**, 2147– 2158.

25 J. Llaveria, Á. Beltrán, W. M. C. Sameera, A. Locati, M. M. Díaz-Requejo, M. I. Matheu, S. Castillón, F. Maseras and P. J. Pérez, *J. Am. Chem. Soc*, 2014, **136**, 5342– 5350.

26 J. Llaveria, Á. Beltrán, M. M. Díaz-Requejo, M. I. Matheu, S. Castillón and P. J. Pérez, *Angew. Chem. Int. Ed*, 2010, **49**, 7092– 7095; *Angew. Chem*, 2010, **122**, 7246.

27 J. R. Gardinier, K. J. Meise, F. Jahan and S. V. Lindeman, *Inorg. Chem*, 2018, **57**, 1572– 1589.

28 J. M. Muñoz-Molina, T. R. Belderrain and P. J. Pérez, *Coord. Chem. Rev*, 2019, **390**, 171– 189.

29 M. Wathier and J. A. Love, *Eur. J. Inorg. Chem*, 2016, **2016**, 2391– 2402.

30 L. M. D. R. S. Martins, *Catalysts*, 2017, **7**, 12.

31 H. R. Bigmore, S. C. Lawrence, P. Mountford and C. S. Tredget, *Dalton Trans*, 2005, 635– 651.

32 L. M. D. R. S. Martins, *Coord. Chem. Rev*, 2019, **396**, 89– 102.

33 L. Maestre, M. R. Fructos, M. M. Díaz-Requejo and P. J. Pérez, *Organometallics*, 2012, **31**, 7839– 7843.

34 D. Macikenas, E. Skrzypczak-Jankun and J. D. Protasiewicz, *J. Am. Chem. Soc*, 1999, **121**, 7164– 7165.

35 L. K. Peterson, E. Kiehlmann, A. R. Sanger and K. I. Thé, *Can. J. Chem*, 1974, **52**, 2367– 2374.

36 K. I. The, L. K. Peterson and E. Kiehlmann, *Can. J. Chem*, 1973, **51**, 2448– 2451.

37 K. I. Thé and L. K. Peterson, *Can. J. Chem*, 1973, **51**, 422– 426.

38 K. I. Thé and L. K. Peterson, *J. Chem. Soc., Chem. Commun.* 1972, 841a– 841a.

39 J. R. Gardinier, A. R. Treleven, K. J. Meise and S. V. Lindeman, *Dalton Trans*, 2016, **45**, 12639– 12643.

40 M. H. Reineke, M. D. Sampson, A. L. Rheingold and C. P. Kubiak, *Inorg. Chem*, 2015, **54**, 3211– 3217.

41 L. Yang, D. R. Powell and R. P. Houser, *Dalton Trans*, 2007, 955– 964.

42 D. L. Reger, J. E. Collins, A. L. Rheingold and L. M. Liable-Sands, *Organometallics*, 1996, **15**, 2029– 2032.

43 K. Fujisawa, T. Ono, Y. Ishikawa, N. Amir, Y. Miyashita, K. Okamoto and N. Lehnert, *Inorg. Chem*, 2006, **45**, 1698– 1713.

44 E. Haldón, E. Álvarez, M. C. Nicasio and P. J. Pérez, *Inorg. Chem*, 2012, **51**, 8298– 8306.

45 A. R. Choudhury and T. N. Guru Row, *Cryst. Growth Des*, 2004, **4**, 47– 52.

46 J.-A. van den Berg and K. R. Seddon, *Cryst. Growth Des*, 2003, **3**, 643– 661.

47 L. Brammer, E. A. Bruton and P. Sherwood, *New J. Chem*, 1999, **23**, 965– 968.

48 V. R. Thalladi, H.-C. Weiss, D. Bläser, R. Boese, A. Nangia and G. R. Desiraju, *J. Am. Chem. Soc*, 1998, **120**, 8702– 8710.

49 F. Grepioni, G. Cojazzi, S. M. Draper, N. Scully and D. Braga, *Organometallics*, 1998, **17**, 296– 307.

50 C.-C. Chou, C.-C. Su, H.-L. Tsai and K.-H. Lii, *Inorg. Chem*, 2005, **44**, 628– 632.

51 K. Fujisawa, Y. Noguchi, Y. Miyashita, K. Okamoto and N. Lehnert, *Inorg. Chem*, 2007, **46**, 10607– 10623.

52 B. Baytekin, H. T. Baytekin and C. A. Schalley, *Org. Biomol. Chem*, 2006, **4**, 2825– 2841.

53 H. N. Miras, E. F. Wilson and L. Cronin, *Chem. Commun*, 2009, 1297– 1311.

54 C. A. Schalley, *Mass Spectrom. Rev*, 2001, **20**, 253– 309.

55 J. A. Loo, *Int. J. Mass Spectrosc*, 2000, **200**, 175– 186.

56 R. D. Smith and K. J. Light-Wahl, *Biol. Mass Spectrom*, 1993, **22**, 493– 501.

57 S. Banerjee and S. Mazumdar, *Int. J. Anal. Chem*, 2012, **2012**, 1– 40.

58 N. C. Habermehl, P. M. Angus, N. L. Kilah, L. Norén, A. D. Rae, A. C. Willis and S. B. Wild, *Inorg. Chem*, 2006, **45**, 1445– 1462.

59 A. M. Camp, M. R. Kita, J. Grajeda, P. S. White, D. A. Dickie and A. J. M. Miller, *Inorg. Chem*, 2017, **56**, 11141– 11150.

60 W. M. Ward, B. H. Farnum, M. Siegler and G. J. Meyer, *J. Phys. Chem. A*, 2013, **117**, 8883– 8894.

61 E. Kleinpeter, A. Koch, H. S. Sahoo and D. K. Chand, *Tetrahedron*, 2008, **64**, 5044– 5050.

62 H. S. Sahoo, D. K. Chand, S. Mahalakshmi, Md. Hedayetullah Mir and R. Raghunathan, *Tetrahedron Lett*, 2007, **48**, 761– 765.

63 A. Macchioni, *Chem. Rev*, 2005, **105**, 2039– 2074.

64 G. N. La Mar, *J. Chem. Phys*, 1964, **41**, 2992– 2998.

65 J. Ammer, C. Nolte, K. Karaghiosoff, S. Thallmair, P. Mayer, R. de Vivie-Riedle and H. Mayr, *Chem. Eur. J*, 2013, **19**, 14612– 14630.

66 K. E. Aldrich, B. S. Billow, D. Holmes, R. D. Bemowski and A. L. Odom, *Organometallics*, 2017, **36**, 1227– 1237.

67 J. R. Gardinier, H. M. Tatlock, J. S. Hewage and S. V. Lindeman, *Cryst. Growth Des*, 2013, **13**, 3864– 3877.

68 J. R. Gardinier, K. J. Meise, F. Jahan, D. Wang and S. V. Lindeman, *Inorg. Chem*, 2019, **58**, 8953– 8968.

69 M. Casarin, D. Forrer, F. Garau, L. Pandolfo, C. Pettinari and A. Vittadini, *J. Phys. Chem. A*, 2008, **112**, 6723– 6731.

70 M. Casarin, D. Forrer, F. Garau, L. Pandolfo, C. Pettinari and A. Vittadini, *Inorg. Chim. Acta*, 2009, **362**, 4358– 4364.

71 H. Takahashi, S. Tsuboyama, Y. Umezawa, K. Honda and M. Nishio, *Tetrahedron*, 2000, **56**, 6185– 6191.

72 Y. Umezawa, S. Tsuboyama, K. Honda, J. Uzawa and M. Nishio, *Bull. Chem. Soc. Jap*, 1998, **71**, 1207– 1213.

73 D. Braga, F. Grepioni and E. Tedesco, *Organometallics*, 1998, **17**, 2669– 2672.

74 S. Tsuzuki, K. Honda, T. Uchimaru, M. Mikami and K. Tanabe, *J. Am. Chem. Soc*, 2000, **122**, 11450– 11458.

75 T. Ozawa, T. Kurahashi and S. Matsubara, *Synlett*, 2013, **24**, 2763– 2767.

76 I. V. Nelson, R. C. Larson and R. T. Iwamoto, *J. Inorg. Nucl. Chem*, 1961, **22**, 279– 284.

77 M. Ignaczak and A. Grzejdziak, *Monatsh. Chem*, 1986, **117**, 1123– 1132.

78 M. L. Tracy and C. P. Nash, *J. Phys. Chem*, 1985, **89**, 1239– 1242.

79 Y. H. Budnikova, Y. B. Dudkina and M. N. Khrizanforov, *Inorganics*, 2017, **5**, 70.

80 H. G. Roth, N. A. Romero and D. A. Nicewicz, *Synlett*, 2016, **27**, 714– 723.

81 D. Bao, B. Millare, W. Xia, B. G. Steyer, A. A. Gerasimenko, A. Ferreira, A. Contreras and V. I. Vullev, *J. Phys. Chem. A*, 2009, **113**, 1259– 1267.

82 CrysAlisPro, Agilent Technologies, 2010.

83 O. V. Dolomanov, L. J. Bourhis, R. J. Gildea, J. A. K. Howard and H. Puschmann, *J. Appl. Crystallogr*, 2009, **42**, 339– 341.

84 G. M. Sheldrick, SHELXTL, Bruker Analytical X-ray Systems, Inc., Madison Wisconsin, USA, 2001.